On Media-based Modulation using RF Mirrors

Y. Naresh, *Student Member, IEEE* and A. Chockalingam, *Senior Member, IEEE*

***Abstract*—Media-based modulation (MBM) is a recently proposed modulation scheme which uses radio frequency (RF) mirrors at the transmit antenna(s) in order to create different channel fade realizations based on their ON/OFF status. These complex fade realizations constitute the modulation alphabet. MBM has the advantage of increased spectral efficiency and performance. In this paper, we investigate the performance of some physical layer techniques when applied to MBM. Particularly, we study the performance of i) MBM with generalized spatial modulation (GSM), ii) MBM with mirror activation pattern (MAP) selection based on an Euclidean distance (ED) based metric, and iii) MBM with feedback based phase compensation and constellation rotation. Our results show that, for the same spectral efficiency, GSM-MBM can achieve better performance compared to MIMO-MBM. Also, it is found that MBM with ED-based MAP selection results in improved bit error performance, and that phase compensation and MBM constellation rotation increases the ED between the MBM constellation points and improves the performance significantly. We also analyze the diversity orders achieved by the ED-based MAP selection scheme and the phase compensation and constellation rotation (PC-CR) scheme. The diversity orders predicted by the analysis are validated through simulations.**

keywords: *Media-based modulation (MBM), RF mirrors, mirror activation pattern (MAP), MIMO-MBM, GSM-MBM, MAP selection, phase compensation, constellation rotation.*

I. Introduction

Traditionally, symbols chosen from complex modulation alphabets like quadrature amplitude modulation (QAM) and phase shift keying (PSK) are used to convey information bits, and complex fades introduced by the channel are viewed as detrimental effects that cause amplitude and phase distortion to the transmitted symbols. An alternate and interesting approach is to consider the complex channel fade coefficients themselves to constitute a modulation alphabet. One simple and known example of this approach is space shift keying (SSK) [1],[2], which can be briefly explained as follows.

1) SSK: Suppose there are two transmit antennas and one receive antenna. Assume rich scattering. Let $h_1 \sim \mathcal{CN}(0,1)$ and $h_2 \sim \mathcal{CN}(0,1)$ denote the complex channel fade coefficients from transmit antennas 1 and 2, respectively, to the receive antenna. Now, assuming that a tone of unit amplitude is transmitted by any one of the transmit antennas in a given channel use, $\mathbb{H} \triangleq \{h_1, h_2\}$ can be viewed as the underlying modulation alphabet, i.e., h_1 and h_2 are the *random* constellation points. The alphabet $\mathbb{H}$ therefore can convey $\log_2 |\mathbb{H}| = \log_2 2 = 1$ information bit. To realize this, if the information bit is 0, antenna 1 transmits the tone and antenna 2 remains silent, and if the information bit is 1, antenna 1 remains silent and antenna 2 transmits the tone. For this, it is enough to have only one transmit radio frequency (RF) chain, whose output is switched to either antenna 1 or antenna 2 depending on the information bit being 0 or 1, respectively. The modulation alphabet (i.e., $\mathbb{H}$) needs to be known at the receiver for detection, which can be obtained through pilot transmission and channel estimation. Note, however, that the transmitter need not know the alphabet $\mathbb{H}$. The information bit is detected using the estimated $\mathbb{H}$ at the receiver.

Similar to the binary SSK scheme with $|\mathbb{H}| = 2$ described above, higher-order SSK with $|\mathbb{H}| = n_t$ and $\mathbb{H} = \{h_1, h_2, \cdots, h_{n_t}\}$ can be realized using $n_t = 2^m$ transmit antennas, and sending the tone on an antenna chosen based on m information bits. Therefore, using $n_t = 2^m$ transmit antennas, SSK achieves a throughput of $m = \log_2 n_t$ bits per channel use (bpcu).

If the receiver has n_r receive antennas, then the alphabet $\mathbb{H}$ will consist of vector constellation points, i.e., $\mathbb{H} = \{\mathbf{h}_1, \mathbf{h}_2, \cdots, \mathbf{h}_{n_t}\}$, where $\mathbf{h}_j = [h_{1,j}\ h_{2,j}\ \cdots\ h_{n_r,j}]^T$, and $h_{i,j} \sim \mathcal{CN}(0,1)$ is the channel fade coefficient from jth transmit antenna to ith receive antenna (see Fig. 1(a)). Because of the increased dimensionality of the constellation points for increasing n_r, the performance of SSK improves significantly with increasing n_r. SSK has the advantages of i) requiring only one transmit RF chain and a $1 \times n_t$ RF switch for any n_t, and ii) yielding attractive performance at higher spectral efficiencies. A key drawback, however, is that SSK needs exponential increase in number of transmit antennas to increase the spectral efficiency. For example, to achieve $m = 8$ bpcu, SSK requires $n_t = 2^8 = 256$ transmit antennas. This drawback of the need to have a large number of transmit antennas to increase the spectral efficiency is significantly alleviated in the recently proposed media-based modulation (MBM) scheme [3]-[7], realized through the use of RF mirrors which are turned ON/OFF[1] on a channel use-by-channel use basis depending on information bits to 'modulate' the fade coefficients of the channel [7]. The basic MBM can be briefly explained as follows.

2) MBM: The basic version of MBM, like SSK, transmits a tone and uses the complex channel fade realizations themselves as the modulation alphabet [3]-[5]. While multiple transmit antennas are needed to create the complex fade

Manuscript received March 28, 2016; revised August 16, 2016, October 5, 2016; accepted October 21, 2016. This work was presented in part at the 2016 Information Theory and Applications Workshop, San Diego, USA, Feb. 2016. The review of this paper was coordinated by Dr. Huiling Zhu.

This work was supported in part by the J. C. Bose National Fellowship, Department of Science and Technology, Government of India.

The authors are with the Department of Electrical Communication Engineering, Indian Institute of Science, Bangalore 560012, India (e-mail: ynr0109434@gmail.com, achockal@ece.iisc.ernet.in).

[1]An RF mirror in ON status implies that the mirror allows the incident wave to pass through it transparently, and an OFF status implies that the mirror reflects back the incident wave.

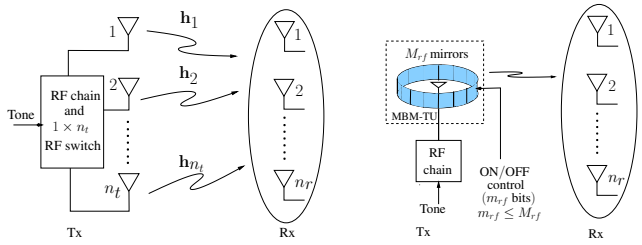

(a) SSK (b) MBM

Fig. 1. (a) SSK with constellation $\mathbb{H}_{\text{ssk}} = \{\mathbf{h}_1, \mathbf{h}_2, \cdots, \mathbf{h}_{n_t}\}$. (b) MBM with constellation $\mathbb{H}_{\text{mbm}} = \{\mathbf{h}_1, \mathbf{h}_2, \cdots, \mathbf{h}_{2^{m_{rf}}}\}$.

symbols of the alphabet in SSK, MBM creates the complex fade symbols of the alphabet even with a single transmit antenna through the use of multiple RF mirrors [7]. This is achieved by placing a number of RF mirrors near the transmit antenna which transmits a tone. Placing RF mirrors near a transmit antenna is equivalent to placing scatterers in the propagation environment close to the transmitter. The radiation characteristics of each of these scatterers (i.e., RF mirrors) can be changed by an ON/OFF control signal applied to it; it reflects back the incident wave originating from the transmit antenna or passes the wave depending on whether it is OFF or ON, respectively. We call the ON/OFF status of the mirrors as the 'mirror activation pattern'. The positions of the ON mirrors and OFF mirrors change from one mirror activation pattern (MAP) to the other, i.e., the propagation environment close to the transmitter changes from one MAP to the other MAP. Note that in a rich scattering environment, since a small perturbation in the propagation environment will be augmented by many random reflections resulting in an independent channel. The RF mirrors create such perturbations by acting as controlled scatterers, which, in turn, create independent fade realizations for different MAPs.

Consider a single transmit antenna. Let M_{rf} denote the total number of RF mirrors placed near the antenna. We call the unit comprising of a transmit antenna and the set of M_{rf} RF mirrors associated with it as the 'MBM transmit unit (MBM-TU)' (see Fig. 1(b)). Out of the M_{rf} available RF mirrors, let m_{rf}, where $1 \leq m_{rf} \leq M_{rf}$, denote the number of RF mirrors actually used. Each of these m_{rf} mirrors is turned ON or OFF in a given channel use based on one information bit. A realization of the ON/OFF status of all the m_{rf} mirrors, determined by m_{rf} information bits, is called a mirror activation pattern (MAP). Therefore, $2^{m_{rf}}$ MAPs are possible. Each of these patterns results in a different realization of the channel fade, resulting in an MBM alphabet of size $|\mathbb{H}| = 2^{m_{rf}}$. Therefore, MBM can convey m_{rf} information bits in one channel use, where m_{rf} is the number of RF mirrors used. That is, the spectral efficiency in MBM scales linearly with the number of RF mirrors used. Note that the spectral efficiency in SSK scales logarithmically in the number of transmit antennas n_t, given by $\lfloor \log_2 n_t \rfloor$ bpcu. In generalized SSK (GSSK) [6], where n_{rf} out of n_t antennas are activated using n_{rf} RF chains, the spectral efficiency increases more than logarithmically and less than linearly in n_t, given by $\lfloor \log_2 \binom{n_t}{n_{rf}} \rfloor$ bpcu. As in SSK, in MBM also the alphabet $\mathbb{H}$ needs to be known at the receiver and not at the transmitter.

MBM has been shown to achieve significant performance gains compared to conventional modulation schemes [3]-[5]. Even with a single transmit antenna and n_r receive antennas, MBM has been shown to achieve significant energy savings compared to a conventional $n_r \times n_t$ MIMO system with $n_r = n_t$ [3]. It has also been shown that MBM with 1 transmit and n_r receive antennas over a static multipath channel asymptotically achieves the capacity of n_r parallel AWGN channels [4]. Implementation of an MBM-TU consisting of $M_{rf} = 14$ RF mirrors placed in a compact cylindrical structure with a dipole transmit antenna element placed at the center of the cylindrical structure has been reported in [7].

We note that the MBM alphabet $\mathbb{H}$ has to be estimated a priori at the receiver. This is achieved through pilot transmissions. Since the number of complex fade symbols to be estimated is $n_{tu}2^{m_{rf}}$, the number of pilot channel uses needed grows exponentially in m_{rf}. Channel sounding to learn the alphabet a priori, therefore, is a key issue in MBM.

3) SM, GSM, MIMO: The need to exponentially increase the number of transmit antennas to increase the spectral efficiency in SSK can be alleviated by allowing the transmission of an M-ary QAM/PSK symbol on the chosen antenna instead of a tone. This allows an additional $\log_2 M$ bits to be conveyed per channel use by the QAM/PSK symbol. This scheme is called the spatial modulation (SM) scheme, which achieves a spectral efficiency of $\log_2 n_t + \log_2 M$ bpcu [8],[9],[10]. A further generalization is to use more than one transmit RF chain (say, n_{rf} transmit RF chains, $1 \leq n_{rf} \leq n_t$), and transmit n_{rf} QAM/PSK symbols through these RF chains. This scheme is called as the generalized spatial modulation (GSM) scheme, whose spectral efficiency is given by $\lfloor \log_2 \binom{n_t}{n_{rf}} \rfloor + n_{rf} \log_2 M$ bpcu [11],[12],[13]. For $n_{rf} = n_t$, the GSM scheme specializes to the well known MIMO (spatial multiplexing) scheme, whose spectral efficiency is given by $n_t \log_2 M$ bpcu. SM systems in frequency-selective channels have been studied in [14]-[16]. The design of SM systems for frequency-selective channels has been summarized in [17], which also discusses SM variants like single-carrier SM (SC-SM), SC-GSM, orthogonal frequency division multiplexing SM (OFDM-SM), space and time-dispersion modulation (STdM), and space-frequency shift keying (SFSK).

4) SM-MBM, GSM-MBM, MIMO-MBM: Multiple MBM-TUs (i.e., multiple transmit antennas, each having its own set of RF mirrors) can be used to increase the spectral efficiency in MBM. Also, like QAM/PSK symbols (as in SM) and additional transmit RF chains (as in GSM, MIMO) could be used to increase the spectral efficiency beyond that can be achieved using SSK, one could use a similar approach to increase the spectral efficiency beyond that can be achieved using the basic MBM. Spatial modulation when used with MBM is referred to as the SM-MBM scheme, whose spectral efficiency is given by $m_{rf} + \lfloor \log_2 n_{tu} \rfloor + \log_2 M$ bpcu, where n_{tu} is the number of MBM-TUs. Similarly, GSM and MIMO (spatial multiplexing) when used with MBM are called GSM-MBM and MIMO-MBM, respectively. The spectral efficiency of GSM-MBM is given by $n_{rf} m_{rf} + \lfloor \log_2 \binom{n_{tu}}{n_{rf}} \rfloor + n_{rf} \log_2 M$ bpcu. The spectral efficiency of MIMO-MBM is given by $n_{tu} m_{rf} + n_{tu} \log_2 M$ bpcu. Note that GSM-MBM specializes

to SM-MBM when $n_{tu} > 1$ and $n_{rf} = 1$. In each channel use, GSM-MBM has two levels of indexing, namely, 1) MBM-TU indexing: n_{rf} out of n_{tu} MBM-TUs are selected using $\lfloor \log_2 \binom{n_{tu}}{n_{rf}} \rfloor$ bits, and 2) RF mirror indexing: a MAP (ON/OFF status of the mirrors) is selected in each of the selected MBM-TUs using m_{rf} bits. The performance of MIMO-MBM has been studied in [7], where it has been shown that MIMO-MBM can achieve better performance compared to conventional MIMO. GSM-MBM performance has not been studied in [7]. One of our contributions in this paper is to present the performance of GSM-MBM and compare it with that of MIMO-MBM.

5) MBM viewed as an instance of index modulation: MBM can be viewed as an instance of index modulation, where information bits are conveyed through the indices of certain transmit entities that get involved in the transmission. Indexing transmit antennas in multi-antenna systems (e.g., SSK, SM, GSM [1],[2],[8]-[13]), indexing subcarriers in multi-carrier systems [18]-[20], indexing both transmit antennas and subcarriers [21], and indexing precoders [22] are examples of such instances. In this context, MBM also can be viewed as an index modulation scheme, where RF mirrors act as the transmit entities that are indexed to convey information bits. In SM-MBM and GSM-MBM, indexing is done both on the MBM-TUs as well as the RF mirrors in each of the chosen MBM-TUs for transmission.

6) Parasitic elements and reconfigurable antennas: The idea of using parasitic elements external to the antenna (which may include capacitors, varactors or switched capacitors that can adjust the resonance frequency) for the purpose of creating multiple antenna patterns is widely known in the literature [23]-[28]. By adjusting the resonance frequency of the different parasitic elements, different channel states for the signal radiating from the antenna can be realized. The use of parasitic elements for beamforming purposes (i.e., to focus the radiated RF energy in specific directions) has been widely studied [23]. Other applications of parasitic elements reported in the literature include selection/switched diversity [24], base station tracking using switched parasitic antenna array [25], direction of arrival estimation with a single-port parasitic array antenna [26], and reconfigurable antennas [27],[28]. These applications do not index antenna patterns to convey information bits, i.e., they do not use parasitic elements for index modulation purposes. Termed as 'aerial modulation,' the idea of indexing orthogonal antenna patterns (realized using a single antenna surrounded by parasitic elements) to convey information bit(s) in addition to bits conveyed through M-PSK symbol has been studied in [29],[30]. The idea of conveying information bits through antenna pattern indexing has also been highlighted in [31]. MBM in [3]-[5] also, in a similar way, exploits the idea of indexing a multiplicity of channel gain profiles realized by placing RF mirrors around the antenna and allowing information bits to control the transparent/opaque status of these mirrors. Extension of MBM to multiple transmit antennas is studied in [7]. In addition, [3]-[7] also highlight the advantages of such systems like additive properties of information over multiple receive antennas.

7) Contributions in this paper: In this paper, we investigate the performance of some physical layer techniques when applied to MBM [32]. These techniques include generalized spatial modulation, MAP selection (analogous to antenna selection in MIMO systems), and phase compensation and constellation rotation (PC-CR). Our contributions in this paper can be summarized as follows.

- We study the performance of MBM with generalized spatial modulation (referred to as GSM-MBM), and compare its performance with that of MIMO-MBM. Our results show that, for the same spectral efficiency, GSM-MBM can achieve better performance compared to MIMO-MBM. A union bound based upper bound on the average bit error probability (BEP) of GSM-MBM is shown to be tight for moderate-to-high SNRs.
- We investigate a MAP selection scheme based on an Euclidean distance (ED) based metric, and compare its bit error performance with that of a mutual information (MI) based MAP selection scheme. The ED-based MAP selection scheme is found to perform better than the MI-based MAP selection scheme by several dBs. The diversity order achieved by the ED-based MAP selection scheme is shown to be $n_r(2^{M_{rf}} - 2^{m_{rf}} + 1)$, which is validated through simulations as well.
- We investigate a scheme with feedback based phase compensation and MBM constellation rotation, which increases the ED between the constellation points and improves the bit error performance significantly. The diversity order achieved by this scheme is shown to be $n_r(n_{tu}+1)$, which is also validated through simulations.

The rest of this paper is organized as follows. Section II presents the GSM-MBM scheme. Section III presents the ED-based MAP selection scheme and its diversity analysis. Section IV presents the feedback based PC-CR scheme and its diversity analysis. Section V presents the results and discussions. Conclusions are presented in VI.

II. GSM-MBM SCHEME

In this section, we introduce the GSM-MBM scheme and analyze its bit error performance. The GSM-MBM transmitter is shown in Fig. 2. It consists of n_{tu} MBM-TUs, n_{rf} transmit RF chains, $1 \leq n_{rf} \leq n_{tu}$, and an $n_{rf} \times n_{tu}$ RF switch. In each MBM-TU, m_{rf} RF mirrors are used. In GSM-MBM, information bits are conveyed using MBM-TU indexing, RF mirror indexing, and QAM/PSK symbols, as follows. In each channel use, $i)$ n_{rf} out of n_{tu} MBM-TUs are selected using $\lfloor \log_2 \binom{n_{tu}}{n_{rf}} \rfloor$ bits, $ii)$ on the selected n_{rf} MBM-TUs, n_{rf} M-ary QAM/PSK symbols (formed using $n_{rf} \log_2 M$ bits) are transmitted, and $iii)$ the ON/OFF status of the m_{rf} mirrors in each of the selected MBM-TU is controlled by m_{rf} bits (so that all the $n_{rf}m_{rf}$ mirrors in the selected n_{rf} MBM-TUs are controlled by $n_{rf}m_{rf}$ bits). Therefore, the achieved rate in bpcu is given by

$$\eta = \underbrace{\left\lfloor \log_2 \binom{n_{tu}}{n_{rf}} \right\rfloor}_{\text{MBM-TU index bits}} + \underbrace{n_{rf}m_{rf}}_{\text{mirror index bits}} + \underbrace{n_{rf} \log_2 M}_{\text{QAM/PSK symbol bits}} \text{ bpcu.} \quad (1)$$

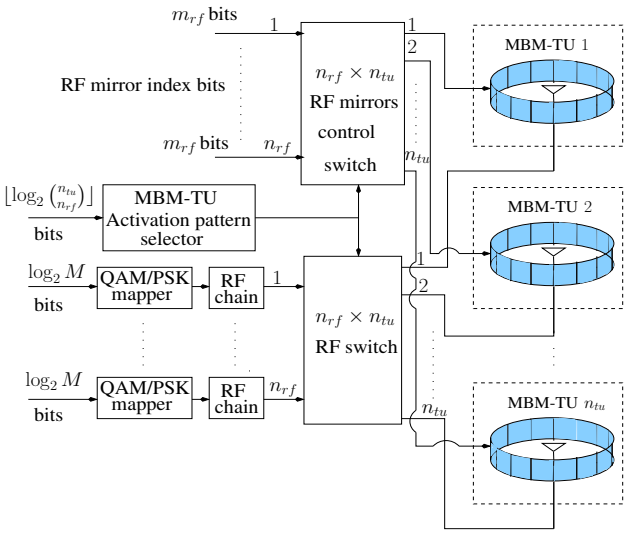

Fig. 2. GSM-MBM transmitter.

GSM-MBM specializes to SIMO-MBM when $n_{tu} = n_{rf} = 1$, to SM-MBM when $n_{tu} > 1$ and $n_{rf} = 1$, and to MIMO-MBM when $n_{tu} > 1$ and $n_{rf} = n_{tu}$.

A. GSM signal set

Let $\mathbb{A}$ denote the M-ary QAM/PSK alphabet used. In a given channel use, each of the n_{tu} MBM-TUs is made ON (and a symbol from $\mathbb{A}$ is sent) or OFF (which is equivalent to sending 0) based on information bits. Let us call a realization of the ON/OFF status of the n_{tu} MBM-TUs as a 'MBM-TU activation pattern'. A total of $\binom{n_{tu}}{n_{rf}}$ MBM-TU activation patterns are possible. Out of them, only $2^{\lfloor \log_2 \binom{n_{tu}}{n_{rf}} \rfloor}$ are needed for signaling. Let $\mathbb{S}_t$ denote the set of these $2^{\lfloor \log_2 \binom{n_{tu}}{n_{rf}} \rfloor}$ MBM-TU activation patterns chosen from the set of all possible MBM-TU activation patterns. A mapping is done between combinations of $\lfloor \log_2 \binom{n_{tu}}{n_{rf}} \rfloor$ bits to MBM-TU activation patterns in $\mathbb{S}_t$. The GSM signal set, denoted by $\mathbb{S}_{\text{gsm}}$, is the set of $n_{tu} \times 1$-sized GSM signal vectors that can be transmitted, which is given by

$$\mathbb{S}_{\text{gsm}} = \left\{ \mathbf{s} : s_j \in \mathbb{A} \cup \{0\},\ \|\mathbf{s}\|_0 = n_{rf},\ \mathcal{I}(\mathbf{s}) \in \mathbb{S}_t \right\}, \tag{2}$$

where $\mathbf{s}$ is the $n_{tu} \times 1$ transmit vector, s_j is the jth entry of $\mathbf{s}$, $j = 1, 2, \cdots, n_{tu}$, $\|\mathbf{s}\|_0$ is the l_0-norm of the vector $\mathbf{s}$, and $\mathcal{I}(\mathbf{s})$ is a function that gives the MBM-TU activation pattern for $\mathbf{s}$. For example, when $\mathbb{A}$ is BPSK, $n_{tu} = 4$ and $n_{rf} = 3$, $\mathbf{s} = [+1 \ \ 0 \ -1 \ -1]^T$ is a valid GSM signal vector, and $\mathcal{I}(\mathbf{s})$ in this case is given by $\mathcal{I}(\mathbf{s} = [+1 \ \ 0 \ -1 \ -1]^T) = [1\ 0\ 1\ 1]^T$.

B. GSM-MBM received signal

In GSM-MBM, in addition to the bits conveyed by the GSM signal vector, the channel fade symbols created by the RF mirrors in the active MBM-TUs also convey additional bits. Let n_r denote the number of receive antennas. Since m_{rf} mirrors are used in each MBM-TU, the number of mirror activation patterns (MAPs) on each MBM-TU is given by $N_m = 2^{m_{rf}}$. Let $\mathbb{S}_m$ denote the set of all N_m MAPs per MBM-TU. Let $\mathbb{H}^j$ denote the MBM alphabet of size N_m, consisting of $n_r \times 1$-sized vector constellation points formed using the channel fade coefficients corresponding to the N_m MAPs of jth MBM-TU to the receive antennas. Let $\mathbf{h}_k^j = [h_{1,k}^j \ h_{2,k}^j \ \cdots \ h_{n_r,k}^j]^T$ denote the $n_r \times 1$-sized channel coefficient vector at the receiver for the kth MAP of the jth MBM-TU, where $h_{i,k}^j$ is the fade coefficient corresponding to the kth MAP of jth MBM-TU to the ith receive antenna, $i = 1, 2, \cdots, n_r$, $j = 1, 2, \cdots, n_{tu}$, and $k = 1, 2, \cdots, N_m$. The $h_{i,k}^j$s are i.i.d. and distributed as $\mathcal{CN}(0, 1)$. We then have $\mathbb{H}^j = \{\mathbf{h}_1^j, \mathbf{h}_2^j, \cdots, \mathbf{h}_{N_m}^j\}$. Let $s_j \in \mathbb{A}$ denote the M-ary QAM/PSK symbol transmitted on the jth MBM-TU. The received signal vector $\mathbf{y} = [y_1 \ y_2 \ \cdots \ y_{n_r}]^T$ in a given channel use is then given by

$$\mathbf{y} = \sum_{j=1}^{n_{tu}} s_j \mathbf{h}_{l_j}^j + \mathbf{n}, \tag{3}$$

where $s_j \in \mathbb{A} \cup \{0\}$, $l_j \in \{1, \cdots, N_m\}$ is the index of the MAP chosen on the jth MBM-TU, $\mathbf{h}_{l_j}^j \in \mathbb{H}^j$, and $\mathbf{n} = [n_1 \ n_2 \ \cdots \ n_{n_r}]^T$ is the additive noise vector, whose elements are i.i.d. and distributed as $\mathcal{CN}(0, \sigma^2)$. Let $\mathbf{H}^j = [\mathbf{h}_1^j \ \mathbf{h}_2^j \ \cdots \ \mathbf{h}_{N_m}^j]$ denote the $n_r \times N_m$ channel matrix corresponding to the jth MBM-TU. The received vector $\mathbf{y}$ in (3) can be written as

$$\mathbf{y} = \sum_{j=1}^{n_{tu}} s_j \mathbf{H}^j \mathbf{e}_{l_j} + \mathbf{n}, \tag{4}$$

where $\mathbf{e}_{l_j}$ is an $N_m \times 1$ vector whose l_jth coordinate is 1 and all other coordinates are zeros. Now, defining $\mathbf{H} = [\mathbf{H}^1 \ \mathbf{H}^2 \ \cdots \ \mathbf{H}^{n_{tu}}]$ as the overall $n_r \times N_m n_{tu}$ channel matrix, we can write $\mathbf{y}$ as

$$\mathbf{y} = \mathbf{H}\mathbf{x} + \mathbf{n}, \tag{5}$$

where $\mathbf{x}$ belongs to the GSM-MBM signal set $\mathbb{S}_{\text{gsm-mbm}}$, which is given by

$$\mathbb{S}_{\text{gsm-mbm}} = \left\{ \mathbf{x} = [\mathbf{x}_1^T \ \mathbf{x}_2^T \ \cdots \ \mathbf{x}_{n_{tu}}^T]^T : \mathbf{x}_j = s_j \mathbf{e}_{l_j}, \right. \\ \left. l_j \in \{1, \cdots, N_m\};\ \ \mathbf{s} = [s_1 \ s_2 \ \cdots \ s_{n_{tu}}]^T \in \mathbb{S}_{\text{gsm}} \right\}. \tag{6}$$

The maximum likelihood (ML) decision rule is given by

$$\hat{\mathbf{x}} = \underset{\mathbf{x} \in \mathbb{S}_{\text{gsm-mbm}}}{\text{argmin}} \ \|\mathbf{y} - \mathbf{H}\mathbf{x}\|^2. \tag{7}$$

The bits corresponding to $\hat{\mathbf{x}}$ are demapped as follows: i) the MBM-TU activation pattern for $\mathbf{s}$ gives $\lfloor \log_2 \binom{n_{tu}}{n_{rf}} \rfloor$ MBM-TU index bits, ii) the non-zero entries in $\mathbf{s}$ gives $n_{rf} \log_2 M$ QAM/PSK bits, and iii) for each non-zero location j in $\mathbf{s}$, l_j gives m_{rf} mirror index bits; since $\mathbf{s}$ has n_{rf} non-zero entries, a total of $n_{rf} m_{rf}$ mirror index bits are obtained from l_j's.

C. Average BEP analysis

The ML decision rule for GSM-MBM is given by (7). The conditional pairwise error probability (PEP) of $\mathbf{x}$ being decoded as $\tilde{\mathbf{x}}$ can be written as

$$P\left(\mathbf{x} \to \tilde{\mathbf{x}} | \mathbf{H}\right) = P\left(\|\mathbf{y} - \mathbf{H}\mathbf{x}\|^2 > \|\mathbf{y} - \mathbf{H}\tilde{\mathbf{x}}\|^2 | \mathbf{H} \right). \tag{8}$$

From (5), we can write (8) as

$$P\left(\mathbf{x} \to \tilde{\mathbf{x}} | \mathbf{H}\right) = P\left(\|\mathbf{n}\|^2 > \|\mathbf{H}\left(\mathbf{x} - \tilde{\mathbf{x}}\right) + \mathbf{n}\|^2 | \mathbf{H} \right)$$

$$= P\big(2\Re\big(\mathbf{n}^{\dagger}\mathbf{H}\left(\tilde{\mathbf{x}}-\mathbf{x}\right)\big) > \|\mathbf{H}\left(\mathbf{x}-\tilde{\mathbf{x}}\right)\|^2|\mathbf{H}\big), \quad (9)$$

where $\Re(.)$ denotes real part, $(.)^{\dagger}$ denotes conjugate transpose, and $2\Re\left(\mathbf{n}^{\dagger}\mathbf{H}\left(\tilde{\mathbf{x}}-\mathbf{x}\right)\right)$ is a Gaussian random variable with zero mean and variance $2\sigma^2\|\mathbf{H}\left(\mathbf{x}-\tilde{\mathbf{x}}\right)\|^2$. Therefore,

$$P\left(\mathbf{x}\rightarrow\tilde{\mathbf{x}}|\mathbf{H}\right) \;=\; Q\Big(\sqrt{\|\mathbf{H}\left(\mathbf{x}-\tilde{\mathbf{x}}\right)\|^2/2\sigma^2}\Big). \quad (10)$$

The computation of the unconditional PEP $P\left(\mathbf{x}\rightarrow\tilde{\mathbf{x}}\right)$ requires the expectation of the $Q\left(.\right)$ function in (10) w.r.t. $\mathbf{H}$, which can be obtained as follows [33]:

$$\begin{aligned} P\left(\mathbf{x}\rightarrow\tilde{\mathbf{x}}\right) &= \mathbb{E}_{\mathbf{H}}\left\{P\left(\mathbf{x}\rightarrow\tilde{\mathbf{x}}|\mathbf{H}\right)\right\} \\ &= \mathbb{E}_{\mathbf{H}}\left\{Q\Big(\sqrt{\|\mathbf{H}\left(\mathbf{x}-\tilde{\mathbf{x}}\right)\|^2/2\sigma^2}\Big)\right\} \\ &= f\left(\beta\right)^{n_r}\sum_{i=0}^{n_r-1}\binom{n_r-1+i}{i}\left(1-f\left(\beta\right)\right)^i, \quad (11) \end{aligned}$$

where $f\left(\beta\right) = \frac{1}{2}\left(1-\sqrt{\frac{\beta}{1+\beta}}\right)$ and $\beta = \frac{\|\mathbf{x}-\tilde{\mathbf{x}}\|^2}{4\sigma^2}$. Now, an upper bound on the average BEP for GSM-MBM based on union bounding can be obtained as

$$P_B \;\leq\; \frac{1}{2^{\eta}}\sum_{\mathbf{x}}\sum_{\tilde{\mathbf{x}}\neq\mathbf{x}} P\left(\mathbf{x}\rightarrow\tilde{\mathbf{x}}\right)\frac{\delta\left(\mathbf{x},\tilde{\mathbf{x}}\right)}{\eta}, \quad (12)$$

where $\delta\left(\mathbf{x},\tilde{\mathbf{x}}\right)$ is the number of bits in which $\mathbf{x}$ differs from $\tilde{\mathbf{x}}$. The BEP upper bound for SIMO-MBM can be obtained from the above expression by setting $n_{tu} = n_{rf} = 1$. Likewise, the BEP upper bound for MIMO-MBM can be obtained by setting $n_{tu} > 1$ and $n_{rf} = n_{tu}$. The bit error rate (BER) performance of GSM-MBM and other multi-antenna schemes are presented in Sec. V-A. Note that the SIMO-MBM, MIMO-MBM, and GSM-MBM schemes do not need any feedback for their operation. In the next two sections, we study how feedback based physical layer techniques can be beneficial when used in MBM schemes.

III. ED-BASED MAP SELECTION

In practice, an MBM-TU may be designed to have more RF mirrors available for use than the number of RF mirrors actually used. Let M_{rf} denote the number of mirrors available in an MBM-TU[2]. This means that the maximum number of channel fade symbols (aka MBM constellation points) that can be generated by the MBM-TU is $2^{M_{rf}}$, i.e., one MBM constellation point per MAP. But not all $2^{M_{rf}}$ MAPs, and hence not all the corresponding MBM constellation points may be used. Only a subset of the $2^{M_{rf}}$ MAPs, say $2^{m_{rf}}$, $m_{rf} \leq M_{rf}$, MAPs are actually used to convey m_{rf} bits through indexing mirrors. Now, one can choose the best subset of $2^{m_{rf}}$ MAPs from the set of all $2^{M_{rf}}$ possible MAPs. In other words, select the best $2^{m_{rf}}$ among the $2^{M_{rf}}$ MBM constellation points and form the MBM alphabet $\mathbb{H}$ of size $|\mathbb{H}| = 2^{m_{rf}}$ constellation points. Such MAP selection in MBM can be viewed as analogous to transmit antenna selection (TAS) in multi-antenna systems, where a subset of antennas among the available antennas is selected for transmission and the selection is based on channel knowledge.

[2]A typical implementation of an MBM-TU reported in the literature has $M_{rf} = 14$ RF mirrors available [7].

Here, we consider MAP selection in MIMO-MBM. Let $\mathbb{S}_{\text{all}}$ denote the set of all possible MAPs per MBM-TU. So, $|\mathbb{S}_{\text{all}}| = 2^{M_{rf}}$. Let $\mathbb{S}_{\text{sub}}$ denote a possible subset of $\mathbb{S}_{\text{all}}$, where $|\mathbb{S}_{\text{sub}}| = 2^{m_{rf}}$, $m_{rf} \leq M_{rf}$. The receiver estimates all the $|\mathbb{S}_{\text{all}}|$ MBM constellation points for every coherence interval, selects the best $|\mathbb{S}_{\text{sub}}|$ constellation points among them, and conveys the indices of the corresponding MAPs to the transmitter. The transmitter uses these selected MAPs to index the mirrors in that coherence interval.

We consider two MAP selection schemes, one that uses an MI-based metric (which is studied in [4],[5]) and another that uses an ED-based metric. ED-based antenna selection has been studied in the context of SM systems in [37]. In [38], an ED-based adaptive spatial modulation (ASM) scheme has been presented, in which the receiver feeds back the most suitable modulation alphabet size for each of the transmit antennas based on the channel estimates for every coherence interval. Also, various link adaptation techniques like transmit precoding and antenna selection based on ED has been summarized in [39], which also summarizes various SM variants like GSSK, GSM, and space-time shift keying (STSK). In what follows in this section, we present MI-based and ED-based MAP selection schemes.

A. MI-based MAP selection

In [4],[5], a selection scheme that chooses the MBM constellation points with the highest energies is studied. This scheme is motivated by the observation that mutual information is proportional to the energy (norm) of the MBM constellation point, and hence selecting the MBM constellation points with the highest energies maximizes the mutual information.

Let $\mathbb{L}^j_{\text{MI}} = \{l_{j1}, l_{j2}, \cdots, l_{j|\mathbb{S}_{\text{sub}}|}\}$ be the set of MAP indices corresponding to the $|\mathbb{S}_{\text{sub}}|$ largest energies for the jth MBM-TU, which expects that

$$\|\mathbf{h}^j_{l_{j1}}\|^2 \geq \|\mathbf{h}^j_{l_{j2}}\|^2 \geq \cdots \geq \|\mathbf{h}^j_{l_{j|\mathbb{S}_{\text{sub}}|}}\|^2 \geq \cdots \geq \|\mathbf{h}^j_{l_{j|\mathbb{S}_{\text{all}}|}}\|^2,$$

$j = 1, 2, \cdots, n_{t_u}$. Let $\mathbb{L}_{\text{MI}} = \{\mathbb{L}^1_{\text{MI}}, \mathbb{L}^2_{\text{MI}}, \ldots, \mathbb{L}^{n_{tu}}_{\text{MI}}\}$ be the set of MAP indices corresponding to all the MBM-TUs. The received signal vector considering this MAP selection is given by

$$\mathbf{y} = \mathbf{H}_{\text{MI}}\mathbf{x} + \mathbf{n}, \quad (13)$$

where $\mathbf{H}_{\text{MI}}$ is the channel matrix of size $n_r \times n_{tu}|\mathbb{S}_{\text{sub}}|$, given by $\mathbf{H}_{\text{MI}} = [\mathbf{H}^1_{\text{MI}}\ \mathbf{H}^2_{\text{MI}}\ \cdots\ \mathbf{H}^{n_{tu}}_{\text{MI}}]$, and $\mathbf{H}^j_{\text{MI}} = [\mathbf{h}^j_{l_{j1}}\ \mathbf{h}^j_{l_{j2}}\ \cdots\ \mathbf{h}^j_{l_{j|\mathbb{S}_{\text{sub}}|}}]$. That is, the selected MBM vector constellation points of all the MBM-TUs form the column vectors of the $\mathbf{H}_{\text{MI}}$ matrix. At the receiver, ML detection is performed using the knowledge of the channel matrix $\mathbf{H}_{\text{MI}}$.

B. ED-based MAP selection

Another way to do MAP selection is to choose the best MBM constellation points based on ED. Let $\mathcal{I}^j$ denote the collection of sets of MAP indices corresponding to the enumerations of the $\binom{|\mathbb{S}_{\text{all}}|}{|\mathbb{S}_{\text{sub}}|}$ combinations of selecting $|\mathbb{S}_{\text{sub}}|$ out of $|\mathbb{S}_{\text{all}}|$ MAPs of the jth MBM-TU. Let $\mathcal{L}$ denote the following set, defined as

$$\mathcal{L} = \left\{\mathbb{L} = \{\mathbb{L}^1, \mathbb{L}^2, \cdots, \mathbb{L}^{n_{tu}}\} : \mathbb{L}^j \in \mathcal{I}^j, j = \{1, \cdots, n_{tu}\}\right\}.$$

Among the $|\mathcal{L}|$ possible sets, choose that set which maximizes the minimum Euclidean distance among all possible transmit vectors. That is,

$$\mathbb{L}_{\text{ED}} = \underset{\mathbb{L}\in\mathcal{L}}{\text{argmax}}\Big\{ \min_{\substack{\mathbf{x},\tilde{\mathbf{x}}\in\mathcal{X}\\ \mathbf{x}\neq\tilde{\mathbf{x}}}} ||\mathbf{H}_{\mathbb{L}}\left(\mathbf{x}-\tilde{\mathbf{x}}\right)||^2\Big\}, \tag{14}$$

where $\mathbf{H}_{\mathbb{L}}$ is the channel matrix of size $n_r \times n_{tu}|\mathbb{S}_{\text{sub}}|$ corresponding to the set $\mathbb{L}$, given by $\mathbf{H}_{\mathbb{L}} = \left[\mathbf{H}_{\mathbb{L}}^1\ \mathbf{H}_{\mathbb{L}}^2\ \cdots\ \mathbf{H}_{\mathbb{L}}^{n_{tu}}\right]$, $\mathbf{H}_{\mathbb{L}}^j = [\mathbf{h}_{l_{j1}}^j\ \mathbf{h}_{l_{j2}}^j\ \cdots\ \mathbf{h}_{l_{j|\mathbb{S}_{\text{sub}}|}}^j]$, l_{j_k} is the kth element in the set $\mathbb{L}^j$, and $\mathcal{X}$ represents the set of all possible transmit vectors. The received signal vector considering this MAP selection is

$$\mathbf{y} \quad = \quad \mathbf{H}_{\mathbb{L}_{\text{ED}}}\mathbf{x} + \mathbf{n}. \tag{15}$$

At the receiver, ML detection is performed using the knowledge of the channel matrix $\mathbf{H}_{\mathbb{L}_{\text{ED}}}$. In Sec. V-B, we present the BER performance of the ED-based and MI-based selection schemes.

Complexity: The order of complexity of MI-based MAP selection scheme per MBM-TU is $\mathcal{O}\left(|\mathbb{S}_{\text{all}}|\right)$. Hence, the order of total complexity is $\mathcal{O}\left(n_{tu}|\mathbb{S}_{\text{all}}|\right)$, which is linear in n_{tu} and $|\mathbb{S}_{\text{all}}|$. Whereas, the order of complexity of ED-based MAP selection in (14) is $\mathcal{O}\left(|\mathcal{L}||\mathcal{X}|^2\right)$, where $|\mathcal{L}| = \binom{|\mathbb{S}_{\text{all}}|}{|\mathbb{S}_{\text{sub}}|}^{n_{tu}}$ and $|\mathcal{X}| = \left(|\mathbb{S}_{\text{sub}}|M\right)^{n_{tu}}$, which is exponential in n_{tu} and $|\mathbb{S}_{\text{all}}|$. Note that complexity in ED-based selection is dependent on M, whereas MI-based selection scheme complexity does not depend on M. The set $\mathcal{L}$ is assumed to be known to both the transmitter and the receiver. If $\mathbb{L}_{\text{MI}}$ in MI based scheme (or $\mathbb{L}_{\text{ED}}$ in ED based scheme) is the kth element in the set $\mathcal{L}$ (i.e., k is the index of the selected set), then the receiver feeds back the integer value k to the transmitter. Since $|\mathcal{L}| = \binom{|\mathbb{S}_{\text{all}}|}{|\mathbb{S}_{\text{sub}}|}^{n_{tu}}$, the number of feedback bits required is $\left\lceil \log_2 \binom{|\mathbb{S}_{\text{all}}|}{|\mathbb{S}_{\text{sub}}|}^{n_{tu}} \right\rceil$.

1) Diversity analysis: In this subsection, we present an analysis of the diversity order achieved by the ED-based MAP selection scheme. We can write $\mathbf{H}_{\mathbb{L}}$ as $\mathbf{H}_{\mathbb{L}} = \mathbf{H}\mathbf{A}_{\mathbb{L}}$, where $\mathbf{H}$ is the channel matrix of size $n_r \times n_{tu}|\mathbb{S}_{\text{all}}|$, given by $\mathbf{H} = \left[\mathbf{H}^1\ \mathbf{H}^2\ \cdots\ \mathbf{H}^{n_{tu}}\right]$, $\mathbf{H}^j = [\mathbf{h}_1^j\ \mathbf{h}_2^j\ \cdots\ \mathbf{h}_{|\mathbb{S}_{\text{all}}|}^j]$, $\mathbf{A}_{\mathbb{L}}$ is the MAP selection matrix of size $n_{tu}|\mathbb{S}_{\text{all}}| \times n_{tu}|\mathbb{S}_{\text{sub}}|$ corresponding to the set $\mathbb{L}$, given by $\mathbf{A}_{\mathbb{L}} = \text{diag}\{\mathbf{A}_{\mathbb{L}^1}, \mathbf{A}_{\mathbb{L}^2}, \cdots, \mathbf{A}_{\mathbb{L}^{n_{tu}}}\}$, and $\mathbf{A}_{\mathbb{L}^j} = [\mathbf{e}_{l_{j1}}\mathbf{e}_{l_{j2}}\cdots\mathbf{e}_{l_{j|\mathbb{S}_{\text{sub}}|}}]$. Note that for every j, $\mathbf{A}_{\mathbb{L}^j}$ can have at most one non-zero element in each row and each column. Now, (14) can be written as

$$\begin{aligned}\mathbb{L}_{\text{ED}} \quad &= \quad \underset{\mathbb{L}\in\mathcal{L}}{\text{argmax}}\Big\{ \min_{\substack{\mathbf{x},\tilde{\mathbf{x}}\in\mathcal{X}\\ \mathbf{x}\neq\tilde{\mathbf{x}}}} ||\mathbf{H}\mathbf{A}_{\mathbb{L}}\left(\mathbf{x}-\tilde{\mathbf{x}}\right)||^2\Big\} \\ &= \quad \underset{\mathbb{L}\in\mathcal{L}}{\text{argmax}}\Big\{ \min_{\substack{\mathbf{z},\tilde{\mathbf{z}}\in\mathcal{X}_{\mathbb{L}}\\ \mathbf{z}\neq\tilde{\mathbf{z}}}} ||\mathbf{H}\left(\mathbf{z}-\tilde{\mathbf{z}}\right)||^2\Big\}, \end{aligned} \tag{16}$$

where $\mathcal{X}_{\mathbb{L}}$ is the set corresponding to $\mathbb{L}$ defined as $\mathcal{X}_{\mathbb{L}} = \{\mathbf{z} : \mathbf{z} = \mathbf{A}_{\mathbb{L}}\mathbf{x}, \mathbf{x} \in \mathcal{X}\}$. Let $\triangle\mathcal{X}_{\mathbb{L}}$ be the set of difference vectors corresponding to the set $\mathcal{X}_{\mathbb{L}}$, i.e., $\triangle\mathcal{X}_{\mathbb{L}} = \{\mathbf{z}-\tilde{\mathbf{z}} : \mathbf{z}, \tilde{\mathbf{z}} \in \mathcal{X}_{\mathbb{L}}, \mathbf{z} \neq \tilde{\mathbf{z}}\}$. Let $\triangle\mathcal{D}$ be the set of matrices defined as

$$\triangle\mathcal{D} = \left\{\mathbf{D} = [\mathbf{d}_1\,\mathbf{d}_2\,\cdots\,\mathbf{d}_{|\mathcal{L}|}] : \mathbf{d}_k \in \triangle\mathcal{X}_{\mathbb{L}_k}, k = 1, \cdots, |\mathcal{L}|\right\},$$

where $\mathbb{L}_k$ is the kth element in the set $\mathcal{L}$. The size of each matrix in $\triangle\mathcal{D}$ is $n_{tu}|\mathbb{S}_{\text{all}}| \times |\mathcal{L}|$. The following proposition gives the diversity order achieved by the ED-based MAP selection scheme in MIMO-MBM.

Proposition 1. *The diversity order achieved by the ED-based MAP selection scheme in MIMO-MBM is given by* $d = n_r\left(|\mathbb{S}_{\text{all}}| - |\mathbb{S}_{\text{sub}}| + 1\right)$.

Proof: The proof is given in Appendix A.

In Sec. V-B, we present the numerical results that validate this Proposition. It can be shown that the diversity order achieved by ED-based MAP selection in GSM-MBM is also given by d. It is further noted that the diversity order for ED-based TAS for SM and V-BLAST systems with ML detection has been analyzed in [40] and [41], respectively, where it has been shown that the diversity order in both these systems is given by $n_r(n_t - n_s + 1)$, where n_t is the total number of available transmit antennas and n_s is the number of selected antennas in TAS.

IV. Phase compensation and constellation rotation

In this section, we study the performance of another feedback based transmission scheme called the *phase compensation and constellation rotation (PC-CR) scheme*. A PC-CR scheme in the context of generalized SSK has been studied in [42]. This scheme exploits the knowledge of the random channel phases (not the amplitudes) at the transmitter to enhance performance. The idea is to co-phase the channels of the active transmit antennas for any spatial-constellation point. That is, the channel phases are compensated at the transmitter, which can be viewed as equal-gain combining (EGC) at the transmitter using knowledge of channel phases at the transmitter. The co-phased spatial-constellation points are further phase-rotated by a deterministic angle which is chosen from $[0, 2\pi)$, so that the minimum Euclidean distance of the constellation points at the receiver is maximized. Here, we study the performance of the PC-CR scheme applied to MIMO-MBM. Consider n_{tu} MBM-TUs at the transmitter, where each MBM-TU uses m_{rf} mirrors. Assume that each MBM-TU transmits a tone.

A. Case of $n_r = 1$

Consider the case when $n_r = 1$. The number of MAPs is $N_m = 2^{m_{rf}}$. For every coherence interval, the receiver estimates all the MBM constellation points, i.e., estimates $h_{1,k}^j$ for every $k \in \{1, 2, \cdots, N_m\}$, $j \in \{1, 2, \cdots, n_{tu}\}$. Let $|h_{1,k}^j|$ and $\phi_{1,k}^j$ denote the magnitude and phase of $h_{1,k}^j$. The receiver feeds back all the phases, i.e., $\phi_{1,k}^j$ for every $k \in \{1, 2, \cdots, N_m\}$, $j \in \{1, 2, \cdots, n_{tu}\}$, to the transmitter. Assume that the feedback is perfect. Using this feedback, the transmitter co-phases (i.e., phase compensates) the channel corresponding to the active MAP in each MBM-TU. Specifically, let $\mathbf{u}$ denote the phase-compensated transmit vector obtained by multiplying the transmit vector $\mathbf{x}$ by phase compensation matrix, given by $\mathbf{W} = \text{diag}\{[(\boldsymbol{\phi}_1^1)^T\ (\boldsymbol{\phi}_1^2)^T\ \cdots (\boldsymbol{\phi}_1^{n_{tu}})^T]\}$, where $\boldsymbol{\phi}_1^j = [e^{-\imath\phi_{1,1}^j}\ e^{-\imath\phi_{1,2}^j}\ \cdots\ e^{-\imath\phi_{1,N_m}^j}]^T$, $j \in \{1, 2, \cdots, n_{tu}\}$, and $\imath = \sqrt{-1}$.

Let $\mathbb{U}_{\text{pc}} \triangleq \{\mathbf{u} : \mathbf{u} = \mathbf{W}\mathbf{x}, \mathbf{x} \in \mathcal{X}\}$, denote the phase-compensated signal set, where $\mathcal{X}$ represents the set of all

possible transmit vectors without phase compensation. After phase compensation, the resultant phase-compensated transmit vectors are further rotated to improve performance. Specifically, denoting the kth vector in $\mathbb{U}_{\text{pc}}$ as $\mathbf{u}_k$, each element in $\mathbf{u}_k$ is rotated by the angle ψ_k. The rotation angles $\{\psi_k\}_{k=1}^{|\mathcal{X}|}$ are chosen such that the minimum Euclidean distance of the constellation at the receiver is maximized. The optimum angles are obtained as the solution to the following optimization problem:

$$\{\hat{\psi_k}\}= \underset{\substack{\psi_k\in[0,2\pi)\\ \forall k}}{\text{argmax}}\Big\{ \min_{\substack{\mathbf{u}_{k_1},\mathbf{u}_{k_2}\in\mathbb{U}_{\text{pc}}\\ k_1\neq k_2}} \|\tilde{\mathbf{h}}_1^T\big(\mathbf{u}_{k_1}e^{\imath\psi_{k_1}} - \mathbf{u}_{k_2}e^{\imath\psi_{k_2}}\big)\|^2\Big\},$$

where $\tilde{\mathbf{h}}_1 = [h_{1,1}^1 \cdots h_{1,N_m}^1 h_{1,1}^2 \cdots h_{1,N_m}^2 \cdots h_{1,1}^{n_{tu}} \cdots h_{1,N_m}^{n_{tu}}]^T$. Taking a geometrical view of the above optimization problem, we can see that its solution is given by $\hat{\psi}_k = (k-1)2\pi/|\mathcal{X}|$.

Let $\mathbb{V}_{\text{pc-cr}}$ denote the resulting signal set after phase compensation and constellation rotation described above. The kth vector in $\mathbb{V}_{\text{pc-cr}}$, denoted by $\mathbf{v}_k$, is then given by $e^{\imath\hat{\psi_k}}\mathbf{u}_k$. The received signal at the receiver can be written as

$$y = \tilde{\mathbf{h}}_1^T\mathbf{v} + n, \tag{17}$$

and the corresponding ML decision rule is given by

$$\hat{\mathbf{v}} = \underset{\mathbf{v}\in\mathbb{V}_{\text{pc-cr}}}{\text{argmin}} |y - \tilde{\mathbf{h}}_1^T\mathbf{v}|^2. \tag{18}$$

Now, from $\hat{\mathbf{v}}$, the detected $\mathbf{x}$ vector, denoted by $\hat{\mathbf{x}}$, can be obtained as $\hat{\mathbf{x}} = (\hat{\mathbf{v}}^\dagger)^T \odot \hat{\mathbf{v}}$, where $\odot$ denotes the element-wise multiplication operator. The $\hat{\mathbf{x}}$ vector is demapped to get the corresponding information bits.

B. Case of $n_r > 1$

When there are more than one receive antenna, the phase compensation presented in the previous subsection for $n_r = 1$ is not directly applicable, since there are $n_r > 1$ complex-valued channels between each MBM-TU and the receiver. Let $\tilde{\mathbf{h}}_k = [h_{k,1}^1 \ \cdots \ h_{k,N_m}^1 \ h_{k,1}^2 \ \cdots \ h_{k,N_m}^2 \cdots \ h_{k,1}^{n_{tu}} \ \cdots \ h_{k,N_m}^{n_{tu}}]^T$ denote the channel coefficient vector of size $N_m n_{tu} \times 1$ of the kth receive antenna, $k = 1, 2, \cdots, n_r$. Here, we present two receiver schemes for phase compensation when $n_r > 1$.

1) Receiver scheme 1: A possible extension of phase compensation for multiple receive antennas ($n_r > 1$) is presented in [43], in which the upper bound on the conditional BEP for the ML decision rule in (18) is evaluated for each receive antenna and the receive antenna with the lowest upper bound is selected. We refer this scheme as receiver scheme 1 (Rx. scheme 1). The upper bound on the conditional BEP (i.e., given $\tilde{\mathbf{h}}_k$) for ML detection in (18) is given by

$$\begin{aligned} P_{B|\tilde{\mathbf{h}}_k} &\leq \frac{1}{2^\eta}\sum_{\mathbf{v}_1}\sum_{\mathbf{v}_2\neq\mathbf{v}_1} P\left(\mathbf{v}_1\to\mathbf{v}_2|\tilde{\mathbf{h}}_k\right)\frac{\delta(\mathbf{v}_1,\mathbf{v}_2)}{\eta} \\ &= \frac{1}{2^\eta}\sum_{\mathbf{v}_1}\sum_{\mathbf{v}_2\neq\mathbf{v}_1} Q\left(\sqrt{\frac{|\tilde{\mathbf{h}}_k^T(\mathbf{v}_1-\mathbf{v}_2)|^2}{2\sigma^2}}\right)\frac{\delta(\mathbf{v}_1,\mathbf{v}_2)}{\eta}. \end{aligned} \tag{19}$$

The receiver selects the receive antenna with lowest upper bound, i.e.,

$$\hat{k} = \underset{k\in\{1,2,\cdots,n_r\}}{\text{argmin}} P_{B|\tilde{\mathbf{h}}_k}. \tag{20}$$

The receiver feeds back all the phases of $\tilde{\mathbf{h}}_{\hat{k}}$. Let $\mathbb{V}_{\text{pc-cr}}^{\hat{k}}$ denote signal set corresponding to the phase compensation and constellation rotation defined as in Sec. IV-A. Only the selected receive antenna (i.e., $\hat{k}$) will be active and others will be silent. The received signal can then be written as

$$y = \tilde{\mathbf{h}}_{\hat{k}}^T\mathbf{v} + n, \tag{21}$$

and the corresponding ML decision rule is given by

$$\hat{\mathbf{v}} = \underset{\mathbf{v}\in\mathbb{V}_{\text{pc-cr}}^{\hat{k}}}{\text{argmin}} |y - \tilde{\mathbf{h}}_{\hat{k}}^T\mathbf{v}|^2. \tag{22}$$

Now, from $\hat{\mathbf{v}}$, the detected $\mathbf{x}$ vector, denoted by $\hat{\mathbf{x}}$, can be obtained as $\hat{\mathbf{x}} = (\hat{\mathbf{v}}^\dagger)^T \odot \hat{\mathbf{v}}$. A drawback in this scheme is that it uses only one antenna to receive signal even though multiple antennas are available at the receiver. To overcome this drawback, we present another possible extension of phase compensation scheme for multiple receive antennas, referred as receiver scheme 2 (Rx. scheme 2) in which signals from all the receive antennas will be used for detection.

2) Receiver scheme 2: The receiver selects the receive antenna for phase compensation as in Sec. IV-B1, and feeds back its corresponding phases to the transmitter. Let $\hat{k}$ denote the selected receive antenna, and let $\mathbb{V}_{\text{pc-cr}}^{\hat{k}}$ denote signal set corresponding to the phase compensation and constellation rotation. The signals from all the receive antennas are used. Then, the received signal vector is given by

$$\mathbf{y} = \mathbf{H}\mathbf{v} + \mathbf{n}, \tag{23}$$

where $\mathbf{H}$ is $n_r \times N_m n_{tu}$ channel matrix given by $\mathbf{H} = [\tilde{\mathbf{h}}_1 \ \tilde{\mathbf{h}}_2 \ \cdots \ \tilde{\mathbf{h}}_{n_r}]^T$. Since phase compensation is carried out based on the phases of $\hat{k}$th receive antenna, the effect of phase compensation needs to be eliminated at other receive antennas. To account for this, we present the modified decision rule as follows:

$$\hat{\mathbf{v}} = \underset{\mathbf{v}\in\mathbb{V}_{\text{pc-cr}}^{\hat{k}}}{\text{argmin}} \|\mathbf{y} - \mathbf{H}^{(\mathbf{v})}\mathbf{v}\|^2, \tag{24}$$

where $\mathbf{H}^{(\mathbf{v})} \triangleq [\tilde{\mathbf{h}}_1^{(\mathbf{v})} \cdots \ \tilde{\mathbf{h}}_{\hat{k}}^{(\mathbf{v})} \cdots \ \tilde{\mathbf{h}}_{n_r}^{(\mathbf{v})}]^T$, and $\tilde{\mathbf{h}}_i^{(\mathbf{v})}$'s are given by

$$\tilde{\mathbf{h}}_i^{(\mathbf{v})} \triangleq \begin{cases} \tilde{\mathbf{h}}_i & \text{if } i = \hat{k} \\ \tilde{\mathbf{h}}_i \odot (\mathbf{v}^\dagger)^T & \text{if } i \neq \hat{k}. \end{cases} \tag{25}$$

Since $\mathbf{x} = (\hat{\mathbf{v}}^\dagger)^T \odot \hat{\mathbf{v}}$, we have $(\tilde{\mathbf{h}}_i^{(\mathbf{v})})^T\mathbf{v} = \tilde{\mathbf{h}}_i^T\mathbf{x}$ for $i \neq \hat{k}$. Now, (24) becomes

$$\begin{aligned} \hat{\mathbf{v}} &= \underset{\mathbf{v}\in\mathbb{V}_{\text{pc-cr}}^{\hat{k}}}{\text{argmin}} |y_{\hat{k}} - \tilde{\mathbf{h}}_{\hat{k}}^T\mathbf{v}|^2 + \sum_{i\neq\hat{k}} |y_i - \tilde{\mathbf{h}}_i^T((\hat{\mathbf{v}}^\dagger)^T \odot \hat{\mathbf{v}})|^2 \\ &= \underset{\mathbf{v}\in\mathbb{V}_{\text{pc-cr}}^{\hat{k}}}{\text{argmin}} |y_{\hat{k}} - \tilde{\mathbf{h}}_{\hat{k}}^T\mathbf{v}|^2 + \sum_{i\neq\hat{k}} |y_i - \tilde{\mathbf{h}}_i^T\mathbf{x}|^2. \end{aligned} \tag{26}$$

From (26), we can see that this decision rule gives the advantage of both phase compensation (by $\hat{k}$th receive antenna) and SNR gain by using other $n_r - 1$ receive antennas.

3) Diversity analysis: In this subsection, we present an analysis of the diversity order achieved by the PC-CR scheme. We present the analysis considering the case of $n_r > 1$ with Rx. scheme 1 at the receiver. A similar analysis applies to Rx. scheme 2 as well as the scheme with $n_r = 1$.

The conditional BEP $P_{B|\tilde{\mathbf{h}}_k}$ in (19) can be approximated by applying the nearest neighbor approximation in the high SNR region ([44], Eq. 5.45), as

$$P_{B|\tilde{\mathbf{h}}_k} \approx Q\left(\sqrt{\frac{1}{2\sigma^2}\min_{\mathbf{v}_1\neq\mathbf{v}_2}|\tilde{\mathbf{h}}_k^T(\mathbf{v}_1-\mathbf{v}_2)|^2}\right)\frac{\delta(\mathbf{v}_1,\mathbf{v}_2)}{\eta}. \quad (27)$$

Let $\tilde{\mathbf{h}} = [\tilde{\mathbf{h}}_1^T \ \tilde{\mathbf{h}}_2^T \ \cdots \ \tilde{\mathbf{h}}_{n_r}^T]^T$ denote the channel coefficient vector of size $N_m n_{tu} n_r \times 1$. Then, we can write $\tilde{\mathbf{h}}_k^T = \tilde{\mathbf{h}}^T\mathbf{B}_k$, where $\mathbf{B}_k$ is the receive antenna selection matrix of size $n_r n_{tu} N_m \times n_{tu} N_m$ corresponding to the kth receive antenna, which is given by $\mathbf{B}_k = [\mathbf{e}_{(k-1)n_{tu}N_m+1} \ \mathbf{e}_{(k-1)n_{tu}N_m+2} \ \cdots \ \mathbf{e}_{kn_{tu}N_m}]$. Now, (20) can be written as

$$\begin{aligned}\hat{k} &= \underset{k\in\{1,\cdots,n_r\}}{\text{argmax}}\left\{\min_{\substack{\mathbf{v}_1,\mathbf{v}_2\in\mathbb{V}^k_{\text{pc-cr}}\\ \mathbf{v}_1\neq\mathbf{v}_2}}|\tilde{\mathbf{h}}_k^T(\mathbf{v}_1-\mathbf{v}_2)|^2\right\}\\ &= \underset{k\in\{1,\cdots,n_r\}}{\text{argmax}}\left\{\min_{\substack{\mathbf{v}_1,\mathbf{v}_2\in\mathbb{V}^k_{\text{pc-cr}}\\ \mathbf{v}_1\neq\mathbf{v}_2}}|\tilde{\mathbf{h}}^T\mathbf{B}_k(\mathbf{v}_1-\mathbf{v}_2)|^2\right\}. \quad (28)\end{aligned}$$

The following proposition gives the diversity order achieved by the PC-CR scheme.

Proposition 2. *The diversity order achieved by the PC-CR scheme is given by* $d_{\text{pc-cr}} = n_r(n_{tu}+1)$.

Proof: The proof is given in Appendix B.

In Sec. V-C, we present the numerical results that validate this Proposition. Section V-C also presents the BER performance of schemes without and with PC-CR.

V. Results and Discussions

The numerical results and discussions for the GSM-MBM scheme (in Sec. II), the MAP selection schemes (in Sec. III), and the PC-CR scheme (in Sec. IV) are presented in this section in Secs. V-A, V-B, and V-C, respectively.

A. Performance of GSM-MBM

1) Comparison between systems with and without RF mirrors: First, in Fig. 3, we illustrate the effectiveness of MBM schemes with RF mirrors compared to other popularly known multi-antenna schemes without RF mirrors. The spectral efficiency is fixed at 8 bpcu for all the schemes considered. All the schemes use $n_r = 16$ and ML detection. The schemes considered are: i) SIMO-MBM with $n_{tu} = n_{rf} = 1$, $m_{rf} = 6$, and 4 QAM (6 bits from indexing RF mirrors and 2 bits from one 4-QAM symbol), ii) MIMO-MBM with $n_{tu} = n_{rf} = 2$, $m_{rf} = 2$, and 4 QAM (4 bits from indexing RF mirrors and 4 bits from two 4-QAM symbols), iii) MIMO (spatial multiplexing) with $n_t = 2$, $n_{rf} = 2$, and 16-QAM (8 bits from two 16-QAM symbols), iv) MIMO (spatial multiplexing) with $n_t = 4$, $n_{rf} = 4$, and 4-QAM (8 bits from four 4-QAM symbols), v) SM with $n_t = 4$, $n_{rf} = 1$, and 64-QAM (2 bits from indexing antennas and 6 bits from one 64-QAM symbol), vi) GSM with $n_t = 4$, $n_{rf} = 2$, and 8-QAM (2 bits from indexing antennas and 6 bits from two 8-QAM symbols), and vii) GSM with $n_t = 4$, $n_{rf} = 3$, and 4-QAM (2 bits from indexing antennas and 6 bits from three 4-QAM symbols). Note that among the above schemes, SIMO-MBM and MIMO-MBM are schemes which use RF mirrors and the others are non-MBM schemes which do not use RF mirrors. It can be seen that the MBM schemes (i.e., SIMO-MBM and MIMO-MBM) with RF mirrors achieve better BER performance compared to other multi-antenna schemes which do not use RF mirrors. The SIMO-MBM and MIMO-MBM schemes perform better than non-MBM schemes because of the use of RF mirror index bits, small QAM size (4-QAM), and no interference ($n_{rf} = 1$ in SIMO-MBM)/less interference ($n_{rf} = 2$ in MIMO-MBM). This illustrates the BER performance advantage possible with systems that employ media-based modulation using RF mirrors. Note that both SIMO-MBM and MIMO-MBM in this example use 4-QAM to achieve 8 bpcu. In this case, SIMO-MBM performs better than MIMO-MBM because there is no spatial interference in SIMO-MBM whereas there is spatial interference in MIMO-MBM. Further note that, since the number of RF mirrors used is more in SIMO-MBM ($m_{rf} = 6$) than in MIMO-MBM ($m_{rf} = 2$), the number of MAPs given by $n_{tu}2^{m_{rf}}$ is more in SIMO-MBM ($1\times 2^6 = 64$) than in MIMO-MBM ($2\times 2^2 = 8$). This means 64 pilot channel uses are needed in SIMO-MBM, whereas only 8 pilot channel uses are needed in MIMO-MBM.

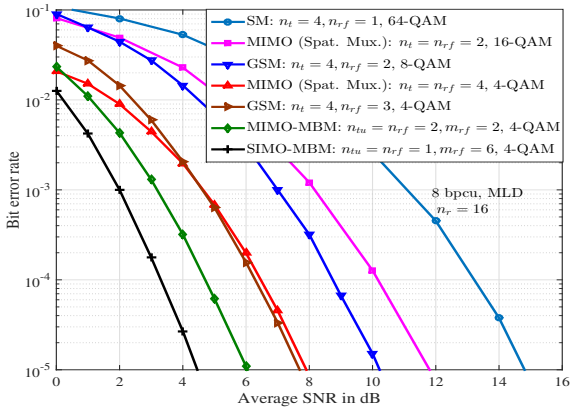

Fig. 3. BER performance comparison between MBM schemes with RF mirrors (SIMO-MBM and MIMO-MBM) and other multi-antenna schemes without RF mirrors (MIMO, SM, GSM) at 8 bpcu and $n_r = 16$.

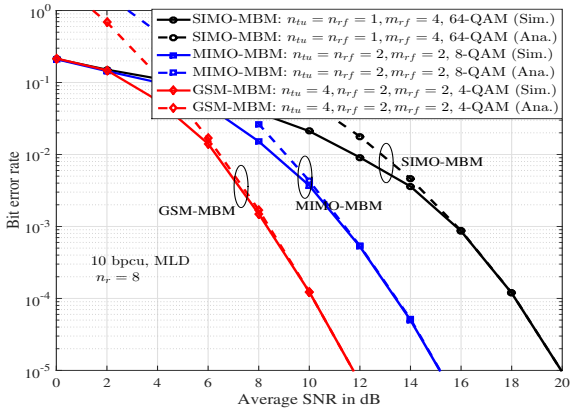

Fig. 4. BER performance of SIMO-MBM, MIMO-MBM, and GSM-MBM with $n_r = 8$, and 10 bpcu. SIMO-MBM: $n_{tu} = n_{rf} = 1$, $m_{rf} = 4$, 64-QAM. MIMO-MBM: $n_{tu} = n_{rf} = 2$, $m_{rf} = 2$, 8-QAM. GSM-MBM: $n_{tu} = 4$, $n_{rf} = 2$, $m_{rf} = 2$, 4-QAM.

2) Comparison between SIMO-MBM, MIMO-MBM, GSM-MBM: Next, we evaluate the BER performance of GSM-MBM scheme through analysis and simulations. We also evaluate the bit error performance of SIMO-MBM and MIMO-MBM schemes for comparison. We compare these three schemes for the same spectral efficiency. Figure 4 shows the BER performance comparison between the following schemes, namely SIMO-MBM, MIMO-MBM, and GSM-MBM schemes, all achieving the same 10 bpcu: i) SIMO-MBM using $n_{tu} = n_{rf} = 1$, $m_{rf} = 4$, and 64-QAM (4 bits from indexing mirrors and 6 bits from one 64-QAM symbol), ii) MIMO-MBM using $n_{tu} = n_{rf} = 2$, $m_{rf} = 2$, and 8-QAM (4 bits from indexing mirrors, 6 bits from two 8-QAM symbols), and iii) GSM-MBM using $n_{tu} = 4$, $n_{rf} = 2$, $m_{rf} = 2$, and 4-QAM (4 bits from indexing mirrors, 2 bits from indexing MBM-TUs, and 4 bits from two 4-QAM symbols). All the three schemes use $n_r = 8$ and ML detection. The following observations can be made from Fig. 4. The analytical upper bound is tight for moderate-to-high SNRs. It is seen that MIMO-MBM achieves better performance compared to SIMO-MBM. For example, at a BER of 10^{-4}, MIMO-MBM requires about 4.4 dB less SNR compared to SIMO-MBM. This is because, although MIMO-MBM has spatial interference, it has the benefit of using a lower QAM size compared to SIMO-MBM (8-QAM in MIMO-MBM and 64-QAM in SIMO-MBM). GSM-MBM is found to perform better than both SIMO-MBM and MIMO-MBM. For example, at 10^{-4} BER, GSM-MBM gives an SNR advantage of about 3.2 dB and 7.8 dB over MIMO-MBM and SIMO-MBM, respectively. This is because more bits are conveyed through indexing in GSM-MBM (i.e., through indexing of mirrors and MBM-TUs), which results in a reduced QAM size (4-QAM for GSM-MBM compared to 8-QAM and 64-QAM for MIMO-MBM and SIMO-MBM, respectively). The results, therefore, show that GSM is an attractive physical layer technique which can be beneficial when used in MBM.

3) Effect of spatial correlation: In the analysis and simulation results presented above, the $h_{i,k}^{j}$s are considered to be i.i.d. However, due to space limitation in the MBM-TU, there can be spatial correlation effects. For example, the channel fades corresponding to different MAPs (i.e., corresponding to the different ON/OFF status of the RF mirrors) in an MBM-TU can be correlated. Likewise, the fades corresponding to the MAPs of different MBM-TUs can also be correlated. Here, we study the effect of these correlations on the performance of MBM. We also present trellis coded modulation (TCM) based symbol mapping to alleviate these correlation effects.

We use the Kronecker model [34], which is commonly used to model spatial correlation. The correlated channel matrix in the Kronecker model is given by

$$\mathbf{H} = \mathbf{R}_{\text{Rx}}^{1/2} \tilde{\mathbf{H}} \mathbf{R}_{\text{Tx}}^{1/2}, \tag{29}$$

where $\mathbf{R}_{\text{Rx}}$ is the $n_r \times n_r$ receive correlation matrix, $\tilde{\mathbf{H}}$ is a matrix of size $n_r \times N_m n_{tu}$ whose entries are i.i.d. and distributed as $\mathcal{CN}(0,1)$, and $\mathbf{R}_{\text{Tx}}$ is the $N_m n_{tu} \times N_m n_{tu}$ transmit correlation matrix. In our system, the transmit correlation matrix is determined by two types of correlation, one among fades across MBM-TUs and another across MAPs in an MBM-TU. The exponentially decaying correlation model [35] is used to characterize the correlation between MBM-TUs, and the equi-correlated model is used to characterize the correlation between fades across MAPs in an MBM-TU. Accordingly, the transmit correlation matrix $\mathbf{R}_{\text{Tx}}$ is written as

$$\mathbf{R}_{\text{Tx}} = \begin{bmatrix} \mathbf{R}_{1,1} & \mathbf{R}_{1,2} & \cdots & \mathbf{R}_{1,n_{tu}} \\ \mathbf{R}_{2,1} & \mathbf{R}_{2,2} & \cdots & \mathbf{R}_{2,n_{tu}} \\ \vdots & \vdots & \ddots & \vdots \\ \mathbf{R}_{n_{tu},1} & \mathbf{R}_{n_{tu},2} & \cdots & \mathbf{R}_{n_{tu},n_{tu}} \end{bmatrix},$$

where $\mathbf{R}_{i,j}$ is an $N_m \times N_m$ matrix whose (k,l)th entry is the correlation coefficient between kth MAP of the ith MBM-TU and lth MAP of the jth MBM-TU. Note that $i = j$ corresponds to correlations across MAPs in an MBM-TU, and $i \neq j$ corresponds to correlations across MBM-TUs. Let ρ_m denote the correlation coefficient in the equi-correlation model in an MBM-TU, i.e., the diagonal elements of $\mathbf{R}_{i,i}$ are 1 and the off-diagonal elements are ρ_m. Let $\rho_a^{|i-j|}$ denote the correlation coefficient in the exponentially decaying correlation model across ith and jth MBM-TUs, i.e., $\mathbf{R}_{i,j}$ for $i \neq j$ is given by $\mathbf{R}_{i,j} = \rho_a^{|i-j|}\mathbf{1}$, where $\mathbf{1}$ represents all ones matrix of size $N_m \times N_m$. Based on the above, the $\mathbf{R}_{\text{Tx}}$ matrix for an example system with $n_{tu} = 3$ and $m_{rf} = 1$ is given by

$$\mathbf{R}_{\text{Tx}} = \left[\begin{array}{cc:cc:cc} 1 & \rho_m & \rho_a & \rho_a & \rho_a^2 & \rho_a^2 \\ \rho_m & 1 & \rho_a & \rho_a & \rho_a^2 & \rho_a^2 \\ \hdashline \rho_a & \rho_a & 1 & \rho_m & \rho_a & \rho_a \\ \rho_a & \rho_a & \rho_m & 1 & \rho_a & \rho_a \\ \hdashline \rho_a^2 & \rho_a^2 & \rho_a & \rho_a & 1 & \rho_m \\ \rho_a^2 & \rho_a^2 & \rho_a & \rho_a & \rho_m & 1 \end{array}\right].$$

The receive correlation matrix $\mathbf{R}_{\text{Rx}}$ is also considered to follow the exponentially decaying correlation model, i.e., the (i,j)th entry of $\mathbf{R}_{\text{Rx}}$ is given by $\rho_a^{|i-j|}$.

In Fig. 5, we illustrate the effect of spatial correlation on the BER performance of GSM-MBM with $n_{tu} = 4$, $n_{rf} = 2$, $m_{rf} = 1$, BPSK, 6 bpcu, and $n_r = 8$. It can be seen that, as would be expected, spatial correlation degrades the BER performance. Higher the correlation, more is the degradation in BER. For example, compared to the system with no correlation (i.e., $\rho_a = \rho_m = 0$), the systems with $\rho_a = \rho_m = 0.3$ and $\rho_a = \rho_m = 0.8$ experience degradation of about 0.5 dB and 7.5 dB, respectively, at 10^{-3} BER. In addition to illustrating the performance degradation due to spatial correlation, this figure also illustrates how trellis coded modulation (TCM) can alleviate this degradation. In [34],[36], bit mapping techniques based on TCM have been proposed to improve the performance of SM systems in the presence of spatial correlation. In [34], only the index bits are convolutionally encoded, whereas both the index and QAM/PSK bits are convolutionally encoded in [36]. Here, we consider a TCM mapping scheme where all the bits are convolutionally encoded as in [36] prior to GSM-MBM encoding. In the TCM coded GSM-MBM scheme the rate is kept the same as 6 bpcu by using TCM with a 64-state trellis convolutional code of rate 6/8 and 4-QAM. The rows of the 6×8 octal generator matrix of the convolutional encoder used are [1 1 1 0 0 0 1 0], [3 1 2 0 0 0 0 0], [2 5 5 0 0 0 0 0], [0 0 0 1 1 1 0 1], [0 0 0 3 1 2 0 0], and [0 0 0 2 5 5 0 0]. A frame size of 20 channel uses and soft decision Viterbi

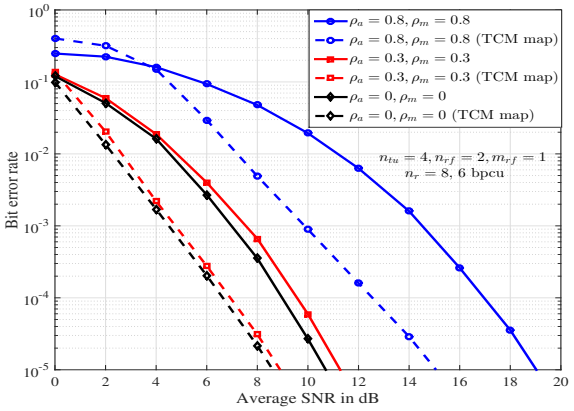

Fig. 5. Effect of spatial correlation on the performance of GSM-MBM with $n_{tu} = 4$, $n_{rf} = 2$, $m_{rf} = 1$, $n_r = 8$, and 6 bpcu. For system with no TCM encoding: BPSK. MLD. For system with TCM encoding: 64-state trellis convolution encoder of rate 6/8, 4-QAM, soft Viterbi decoding.

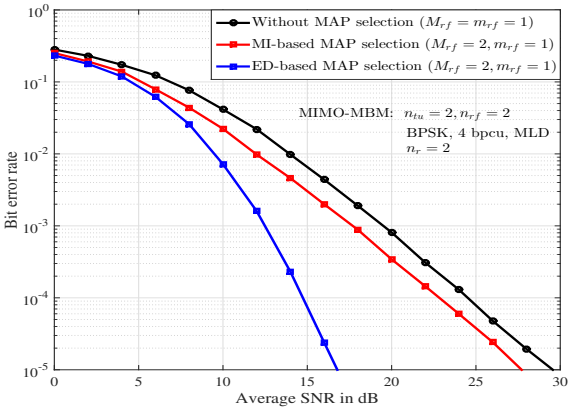

Fig. 6. BER performance comparison between MIMO-MBM schemes without and with MAP selection, $n_{tu} = n_{rf} = 2$, BPSK, 4 bpcu, and $n_r = 2$: i) no MAP selection with $M_{rf} = m_{rf} = 1$, ii) MI-based MAP selection with $M_{rf} = 2$, $m_{rf} = 1$, and iii) ED-based MAP selection with $M_{rf} = 2$, $m_{rf} = 1$.

decoder are used. It can be seen in Fig. 5 that, for the same bpcu, TCM encoding improves the BER performance of GSM-MBM in the presence of spatial correlation. For example, for $\rho_a = \rho_m = 0.3$ and $\rho_a = \rho_m = 0.8$, TCM results in an improvement of about 2.5 dB and 4.5 dB, respectively, at a BER of 10^{-3}. We have observed similar improvements for various combinations of ρ_a and ρ_m values.

B. Performance of MAP selection schemes

In Fig. 6, we present a comparison between the BER performance achieved by MIMO-MBM schemes without and with MAP selection. Three schemes, all with $n_{tu} = n_{rf} = 2$, BPSK, 4 bpcu, and $n_r = 2$, are considered. The first scheme is a scheme with no MAP selection, i.e., $M_{rf} = m_{rf} = 1$. The second scheme is a scheme with MI-based MAP selection where $M_{rf} = 2$ and $m_{rf} = 1$. The third scheme is same as the second scheme, except that MAP selection is done based on ED. In all the three schemes, two bits through BPSK symbols (one bit on each MBM-TU) and two bits through RF mirror indexing (one bit on each MBM-TU) result in 4 bpcu. As expected, we observe that the MAP selection schemes achieve better performance compared to the scheme without MAP selection. This is because of the better minimum distance between constellation points achieved by the selection schemes. We also see that ED-based selection achieves significantly better performance compared to MI-based selection. In fact, ED-based selection achieves a higher diversity order compared to MI-based selection. Again, the reason for this is that, because it maximizes the minimum Euclidean distance, the constellation points chosen by ED-based selection have better minimum distance between them compared those chosen by MI-based selection. This can be observed in Fig. 7, which shows the constellation diagrams for the selection schemes with $n_{tu} = n_{rf} = n_r = 1$, $M_{rf} = 5, m_{rf} = 3$, and BPSK. The minimum distance between the constellation points, d_{min}, are 0.0118, 0.3690, and 0.5263 for the schemes without selection, MI-based selection, and ED-based selection, respectively.

Figure 8 presents a validation of the diversity orders of ED-based selection predicted by Proposition 1. The slopes of the

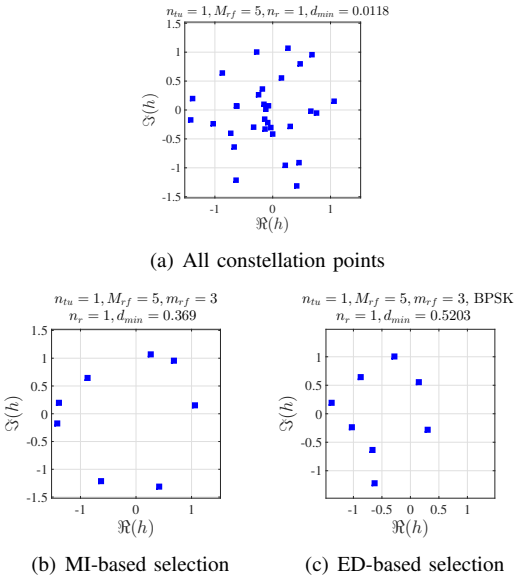

(a) All constellation points

(b) MI-based selection

(c) ED-based selection

Fig. 7. Constellation diagrams without and with MAP selection. (a) Set of all constellation points. (b) Constellation points selected by MI-based selection. (c) Constellation points selected by ED-based selection.

simulated BER plots in the high SNR regime show that the achieved diversity orders are 3 and 6 for the schemes with $M_{rf} = 2$, $m_{rf} = 1$, and $n_r = 1$ and 2, respectively, which are the same as the ones (i.e., $n_r \left(2^{M_{rf}} - 2^{m_{rf}} + 1\right)$) proved analytically by Proposition 1. The constants used in Fig. 8 are $c_1 = 2000$ and $c_2 = 169990$.

We carried out simulations to predict the diversity order of the MI-based selection scheme. The obtained results are shown in Fig. 9. From this figure, it is seen that the diversity order achieved is n_r. The reason for this can be explained as follows. The distance between any two MBM constellation points is a sum of n_r independent random variables, and selecting the constellation points based on energy (i.e., MI) will not change the distance properties. Therefore, the diversity order of the PEPs in which the MAP indices are distinct is n_r, and hence the diversity order of MI-based MAP selection scheme is n_r. The constants used in Fig. 9 are $c_1 = 15$, $c_2 = 9$, $c_3 = 45$, and $c_4 = 17$.

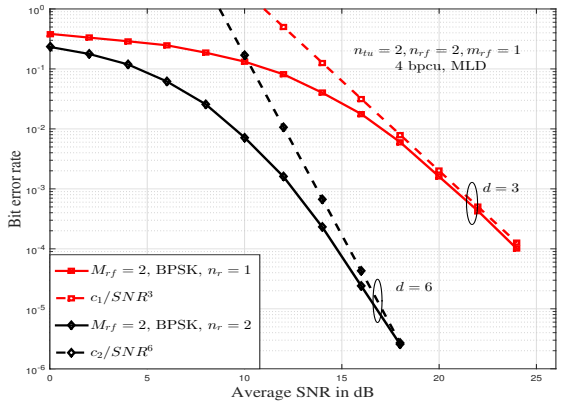

Fig. 8. Diversity orders achieved by ED-based MAP selection in MIMO-MBM for various system parameters.

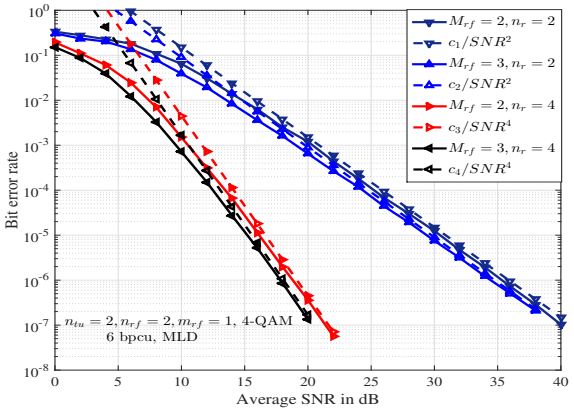

Fig. 9. Diversity orders achieved by MI-based MAP selection in MIMO-MBM with $n_{tu}=n_{rf}=2, m_{rf}=1$, 4-QAM, and 6 bpcu for various values of M_{rf} and n_r: *i)* $M_{rf}=2, n_r=2$; *ii)* $M_{rf}=3, n_r=2$; *iii)* $M_{rf}=2, n_r=4$; *iv)* $M_{rf}=3, n_r=4$.

C. Performance of PC-CR scheme

Figure 10 shows the BER performance of MIMO-MBM without and with PC-CR, for $n_{tu}=n_{rf}=2$, $m_{rf}=1$, tone, 2 bpcu, $n_r=1$, and ML detection. It can be seen that the feedback based PC-CR scheme significantly improves the BER performance; e.g., PC-CR scheme with perfect feedback is found to achieve an improved performance of about 20 dB at 10^{-3} BER compared to the scheme without PC-CR. This is because of the maximization of the minimum ED at the receiver in the PC-CR scheme. Note that the number of phase values to be fed back in the PC-CR scheme is $n_{tu}2^{m_{rf}}$, which is exponential in m_{rf}. To study the effect of limited feedback on the performance of PC-CR, we consider that each feedback phase value is quantized using B bits and these quantized bits are fed back. Since $n_{tu}2^{m_{rf}}$ phase values need to be fed back, the number of feedback bits required is $n_{tu}2^{m_{rf}}B$. Since the phases are uniformly distributed in $(-\pi,\pi]$, the quantization levels are $-\pi+\frac{2\pi k}{2^B}$, $1\le k\le 2^B$. For each feedback phase value, the receiver finds the nearest quantization level and feeds back its corresponding k using B bits to the transmitter. In Fig. 10, we illustrate the effect of number of feedback bits B on the BER performance. It can be seen that the performance with 1-bit feedback is severely degraded, i.e.,

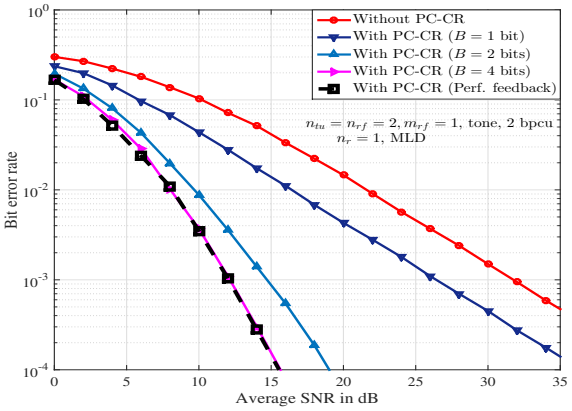

Fig. 10. BER performance of MIMO-MBM without and with PC-CR (perfect feedback and limited feedback) for $n_{tu}=n_{rf}=2$, $m_{rf}=1$, tone, 2 bpcu, $n_r=1$, and ML detection.

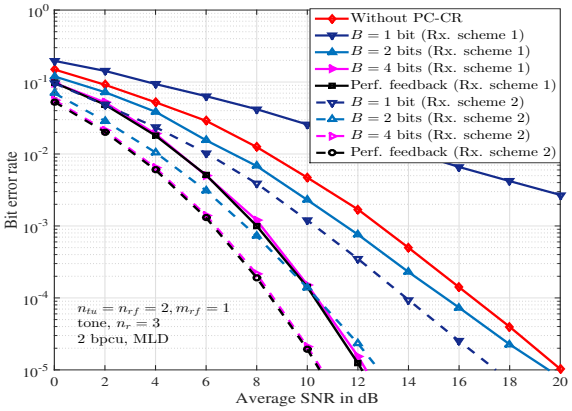

Fig. 11. BER performance of MIMO-MBM without and with PC-CR using Rx. scheme 1 and Rx. scheme 2 for $n_{tu}=n_{rf}=2$, $m_{rf}=1$, tone, 2 bpcu, $n_r=3$, and ML detection.

there is a degradation of about 14 dB at 10^{-3} BER compared to the case of perfect feedback. However, increasing B from 1 bit to 2 bits significantly improves the performance (by about 11 dB at 10^{-3} BER). It can be further noted that with just 4-bit feedback ($B=4$), performance very close to perfect feedback is achieved.

Figure 11 shows the BER performance of MIMO-MBM without and with PC-CR using Rx. scheme 1 and Rx. scheme 2 for $n_{tu}=n_{rf}=2$, $m_{rf}=1$, tone, 2 bpcu, $n_r=3$, and ML detection. This figure also shows the performance with limited feedback for $B=1,2$, and 4 bits per feedback phase. It can be seen that $B=4$-bit feedback is sufficient to achieve performance very close to that with perfect phase feedback. Further it can be seen that the Rx. scheme 2 performs better than Rx. scheme 1 by about 1.5 dB at 10^{-5} BER. This is because Rx. scheme 2 uses signals from all the receive antennas for detection, whereas Rx. scheme 1 uses the signal only from the selected receive antenna.

Figure 12 presents a validation of the diversity orders predicted by Proposition 2. The slopes of the simulated BER plots in the high SNR regime show that the achieved diversity orders are 6, 6, 4, 8, and 7 for the schemes with ($n_{tu}=1$, $m_{rf}=1$, $n_r=3$, 1 bpcu), ($n_{tu}=2$, $m_{rf}=1$, $n_r=2$, 2 bpcu), ($n_{tu}=1$, $m_{rf}=3$, $n_r=2$, 3 bpcu), ($n_{tu}=3$, $m_{rf}=1$,

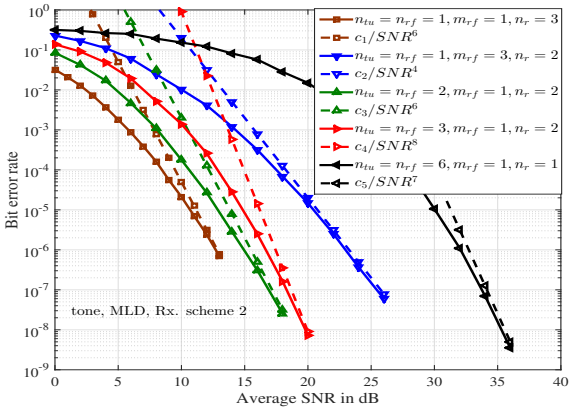

Fig. 12. Diversity orders achieved by MIMO-MBM with PC-CR using Rx. scheme 2 for different system configurations: *i)* $n_{tu}=1, m_{rf}=1, n_r=3$ (1 bpcu); *ii)* $n_{tu}=2, m_{rf}=1, n_r=2$ (2 bpcu); *iii)* $n_{tu}=1, m_{rf}=3, n_r=2$ (3 bpcu); *iv)* $n_{tu}=3, m_{rf}=1, n_r=2$ (3 bpcu); *v)* $n_{tu}=6, m_{rf}=1, n_r=1$ (6 bpcu).

$n_r=2$, 3 bpcu), and ($n_{tu}=6$, $m_{rf}=1$, $n_r=1$, 6 bpcu), respectively, which are the same as the ones obtained from the diversity order given by $n_r(n_{tu}+1)$. The constants used in Fig. 12 are $c_1=50, c_2=2000, c_3=2000, c_4=9\times10^7$, and $c_5=4\times10^7$.

VI. Conclusions

We investigated the performance of some interesting physical layer techniques when applied to media-based modulation (MBM), which is a recently proposed modulation scheme that uses RF mirrors to perturb the propagation environment to create independent channel fade realizations which themselves are used as the constellation points. The considered physical layer techniques included generalized spatial modulation (GSM), mirror activation pattern (MAP) selection (analogous to antenna selection in MIMO systems), and phase compensation and constellation rotation. It was shown that, for the same spectral efficiency, GSM-MBM can achieve better performance compared to MIMO-MBM. The Euclidean distance based MAP selection scheme was found to perform better than the mutual information based MAP selection scheme by several dBs. The diversity order achieved by the Euclidean distance based MAP selection scheme was shown to be $n_r(2^{M_{rf}}-2^{m_{rf}}+1)$, which was also validated through simulations. Feedback based phase compensation and MBM constellation rotation was found to increase the Euclidean distance between the constellation points, thereby improving the bit error performance significantly. The diversity order achieved by the phase compensation and constellation rotation scheme was shown to be $n_r(n_{tu}+1)$, which was validated through simulations.

Appendix A
Proof of Proposition 1

Proof: Let $d_{\mathbf{x},\tilde{\mathbf{x}}}$ denote the diversity order of PEP $P(\mathbf{x}\to\tilde{\mathbf{x}})$. Then, the diversity order (d) achieved by ED-based MAP selection scheme is given by

$$d = \min_{\mathbf{x}\neq\tilde{\mathbf{x}}} d_{\mathbf{x},\tilde{\mathbf{x}}}. \quad (30)$$

Let $\mathbb{L}_{\text{ED}}$ be the k_{ED}th element in the set $\mathcal{L}$. In the following, we derive lower and upper bounds on d and show that both these bounds turn out to be the same, given by $n_r(|\mathbb{S}_{\text{all}}|-|\mathbb{S}_{\text{sub}}|+1)$.

1) Lower bound on d: The conditional PEP between $\mathbf{x}$ and $\tilde{\mathbf{x}}$ is given by

$$\begin{aligned} P(\mathbf{x}\to\tilde{\mathbf{x}}|\mathbf{H}) &= Q\big(\sqrt{\|\mathbf{H}\mathbf{A}_{\mathbb{L}_{\text{ED}}}(\mathbf{x}-\tilde{\mathbf{x}})\|^2/2\sigma^2}\big) \\ &\leq \frac{1}{2}\exp\big(-\|\mathbf{H}(\mathbf{z}-\tilde{\mathbf{z}})\|^2/4\sigma^2\big), \quad (31)\end{aligned}$$

where $\mathbf{z}=\mathbf{A}_{\mathbb{L}_{\text{ED}}}\mathbf{x}, \tilde{\mathbf{z}}=\mathbf{A}_{\mathbb{L}_{\text{ED}}}\tilde{\mathbf{x}}$, $\mathbf{z},\tilde{\mathbf{z}}\in\mathcal{X}_{\mathbb{L}_{\text{ED}}}$, and the inequality in (31) follows from Chernoff bound. For a given $k, k=1,\cdots,|\mathcal{L}|$, let $\mathbf{d}_{\text{min}}(k)$ represent the difference vector in $\Delta\mathcal{X}_{\mathbb{L}_k}$ corresponding to the minimum ED, i.e., $\mathbf{d}_{\text{min}}(k)=\text{argmin}_{d\in\Delta\mathcal{X}_{\mathbb{L}_k}}\|\mathbf{H}\mathbf{d}\|^2$. Let $\mathbf{D}_{\text{min}}$ is the matrix defined as $\mathbf{D}_{\text{min}}=[\mathbf{d}_{\text{min}}(1)\ \mathbf{d}_{\text{min}}(2)\ \cdots\ \mathbf{d}_{\text{min}}(|\mathcal{L}|)]$. Then, we have

$$\|\mathbf{H}(\mathbf{z}-\tilde{\mathbf{z}})\|^2 \geq \|\mathbf{H}\mathbf{d}_{\text{min}}(k_{\text{ED}})\|^2 \quad (32)$$

$$\geq \frac{1}{|\mathcal{L}|}\|\mathbf{H}\mathbf{D}_{\text{min}}\|^2 = \frac{1}{|\mathcal{L}|}\text{Tr}\big(\mathbf{H}\mathbf{D}_{\text{min}}\mathbf{D}_{\text{min}}{}^{\dagger}\mathbf{H}^{\dagger}\big), \quad (33)$$

where $\text{Tr}(.)$ denotes the trace operator, the inequality in (32) follows from the definition of $\mathbf{d}_{\text{min}}(k_{\text{ED}})$, and the inequality in (33) follows from the fact $\|\mathbf{H}\mathbf{d}_{\text{min}}(k_{\text{ED}})\|^2 \geq \|\mathbf{H}\mathbf{d}_{\text{min}}(k)\|^2, 1\leq k\neq k_{\text{ED}}\leq|\mathcal{L}|$. Using eigenvalue decomposition, we have $\mathbf{D}_{\text{min}}\mathbf{D}_{\text{min}}{}^{\dagger}=\mathbf{U}\Lambda\mathbf{U}^{\dagger}$, where $\mathbf{U}$ is a unitary matrix and $\Lambda=\text{diag}\{\lambda_1,\lambda_2,\cdots,\lambda_p,0,0,\cdots,0\}$, $\lambda_i\neq0$, $i=1,\cdots,p$, $p=rank(\mathbf{D}_{\text{min}})$. Then, we have

$$\begin{aligned}\|\mathbf{H}(\mathbf{z}-\tilde{\mathbf{z}})\|^2 &\geq \frac{1}{|\mathcal{L}|}\text{Tr}\big(\tilde{\mathbf{H}}\Lambda\tilde{\mathbf{H}}^{\dagger}\big) = \frac{1}{|\mathcal{L}|}\sum_{i=1}^{n_r}\sum_{j=1}^{p}\lambda_j|\tilde{h}_{i,j}|^2 \\ &\geq \frac{\lambda_{\text{min}}}{|\mathcal{L}|}\sum_{i=1}^{n_r}\sum_{j=1}^{p}|\tilde{h}_{i,j}|^2, \quad (34)\end{aligned}$$

where $\tilde{\mathbf{H}}=\mathbf{H}\mathbf{U}$, $\lambda_{\text{min}}=\min_{\mathbf{D}\in\Delta\mathcal{D}}\lambda_s\big(\mathbf{D}\mathbf{D}^{\dagger}\big)$, and $\lambda_s\big(\mathbf{D}\mathbf{D}^{\dagger}\big)$ is the smallest non-zero eigenvalue of $\mathbf{D}\mathbf{D}^{\dagger}$. Since $\mathbf{U}$ is unitary, the entries of $\tilde{\mathbf{H}}$ are i.i.d. and $\mathcal{CN}(0,1)$. From (31) and (34), we have

$$P(\mathbf{x}\to\tilde{\mathbf{x}}|\mathbf{H}) \leq \frac{1}{2}\exp\left(-\frac{\lambda_{\text{min}}}{4\sigma^2|\mathcal{L}|}\left(\sum_{i=1}^{n_r}\sum_{j=1}^{p}|\tilde{h}_{i,j}|^2\right)\right). \quad (35)$$

The unconditional PEP is then given by

$$P(\mathbf{x}\to\tilde{\mathbf{x}}) \leq \mathbb{E}_{\mathbf{H}}\left\{\frac{1}{2}\exp\left(-\frac{\lambda_{\text{min}}}{4\sigma^2|\mathcal{L}|}\left(\sum_{i=1}^{n_r}\sum_{j=1}^{p}|\tilde{h}_{i,j}|^2\right)\right)\right\}. \quad (36)$$

Since $|\tilde{h}_{i,j}|^2$s are independent and exponentially distributed with unit mean, we have

$$P(\mathbf{x}\to\tilde{\mathbf{x}}) \leq \frac{1}{2}\prod_{i=1}^{n_r}\prod_{j=1}^{p}\left(1+\frac{\lambda_{\text{min}}}{4\sigma^2|\mathcal{L}|}\right)^{-1}. \quad (37)$$

At high SNRs, $\frac{\lambda_{\text{min}}}{4\sigma^2|\mathcal{L}|}\gg1$. Hence, we can write

$$P(\mathbf{x}\to\tilde{\mathbf{x}}) \leq \frac{1}{2}\left(\frac{\lambda_{\text{min}}}{4\sigma^2|\mathcal{L}|}\right)^{-n_rp}. \quad (38)$$

Based on union bound, average BEP at high SNRs can be bounded as

$$P_B \leq \frac{1}{2^{\eta}}\sum_{\mathbf{x}}\sum_{\tilde{\mathbf{x}}\neq\mathbf{x}}P(\mathbf{x}\to\tilde{\mathbf{x}})\frac{\delta(\mathbf{x},\tilde{\mathbf{x}})}{\eta}$$

$$\leq \quad \frac{(2^{\eta}-1)}{2\eta}\Big(\frac{\lambda_{\min}}{4\sigma^2|\mathcal{L}|}\Big)^{-n_r p}, \tag{39}$$

which shows that the diversity order achieved by ED based MAP selection scheme is lower bounded by $n_r p$. Next, we show that $p \geq (|\mathbb{S}_{\text{all}}| - |\mathbb{S}_{\text{sub}}| + 1)$. Any matrix $\mathbf{D} \in \triangle\mathcal{D}$ can be viewed in the form $\mathbf{D} = [\mathbf{D}_1^T \ \mathbf{D}_2^T \ \cdots \ \mathbf{D}_{n_{tu}}^T]^T$, where $\mathbf{D}_j$ is a sub-matrix of size $|\mathbb{S}_{\text{all}}| \times |\mathcal{L}|$. Consider a matrix $\mathbf{D} \in \triangle\mathcal{D}$ which is constrained such that only one sub-matrix (say, $\mathbf{D}_k$) is a non-zero sub-matrix and all other sub-matrices ($\mathbf{D}_j$'s, $j \neq k$) are zero sub-matrices. That is, the constrained matrix is of the form $\mathbf{D} = [\mathbf{0}^T \ \mathbf{0}^T \ \cdots \ \mathbf{D}_k^T \ \cdots \ \mathbf{0}^T \ \mathbf{0}^T]^T$, $k \in \{1, 2, \cdots, n_{tu}\}$. Therefore, $rank(\mathbf{D}) = rank(\mathbf{D}_k)$. Any matrix in $\triangle\mathcal{D}$ which does not have the above constraint can be obtained by replacing one or more zero sub-matrices by non-zero sub-matrices. Since a rank of a matrix will not reduce if some of its zero rows/columns are replaced by non-zero rows/columns, the minimum rank is obtained by matrices with the above constraint. Let $\triangle\mathbb{A}$ denote the set of non-zero difference QAM/PSK constellation points, given by $\{s_1 - s_2 : s_1, s_2 \in \mathbb{A}, s_1 \neq s_2\}$. Note that every column of $\mathbf{D}_k$ is either from the set $\mathcal{E}_l \triangleq \{c\,\mathbf{e}_l : c \in \triangle\mathbb{A}\}$ for $1 \leq l \leq |\mathbb{S}_{\text{all}}|$ or from the set $\mathcal{E}_{l,q} \triangleq \{s_1\mathbf{e}_l - s_2\mathbf{e}_q : s_1, s_2 \in \mathbb{A}\}$ for $1 \leq l \neq q \leq |\mathbb{S}_{\text{all}}|$. Now, using Proposition 2 of [40], the minimum rank of $\mathbf{D}_k$ is $|\mathbb{S}_{\text{all}}| - |\mathbb{S}_{\text{sub}}| + 1$. Hence, $p = rank\,(\mathbf{D}_{\min}) \geq \min\{rank\,(\mathbf{D}) : \mathbf{D} \in \triangle\mathcal{D}\} = |\mathbb{S}_{\text{all}}| - |\mathbb{S}_{\text{sub}}| + 1$. Therefore, d is lower bounded by $n_r p \geq n_r\,(|\mathbb{S}_{\text{all}}| - |\mathbb{S}_{\text{sub}}| + 1)$, i.e.,

$$d \quad \geq \quad n_r\,(|\mathbb{S}_{\text{all}}| - |\mathbb{S}_{\text{sub}}| + 1)\,. \tag{40}$$

2) Upper bound on d: Consider a pair of transmitted vectors $\mathbf{x}$, $\hat{\mathbf{x}}$ such that $\mathbf{x}_1 \neq \hat{\mathbf{x}}_1$, $\mathbf{x}_1 = s_1\mathbf{e}_1, \hat{\mathbf{x}}_1 = \hat{s}_1\mathbf{e}_1$, $\mathbf{x}_i = \hat{\mathbf{x}}_i$, for $2 \leq i \leq n_{tu}$, where $\mathbf{x}_1, \hat{\mathbf{x}}_1, \mathbf{x}_i$, and $\hat{\mathbf{x}}_i$ are defined as in (6). Since we are selecting $|\mathbb{S}_{\text{sub}}|$ out of $|\mathbb{S}_{\text{all}}|$ MAPs, there exist at least one $l_{1i}, i = 1, \cdots, |\mathbb{S}_{\text{sub}}|$ such that $1 \leq l_{1i} \leq p_d$, where $p_d = |\mathbb{S}_{\text{all}}| - |\mathbb{S}_{\text{sub}}| + 1$. Now, we have

$$\begin{aligned}
\|\mathbf{H}\mathbf{A}_{\mathbb{L}_{\text{ED}}}(\mathbf{x} - \hat{\mathbf{x}})\|^2 &= \|\mathbf{H}^1\mathbf{A}_{\mathbb{L}^1_{\text{ED}}}(\mathbf{x}_1 - \hat{\mathbf{x}}_1)\|^2 && (41)\\
&\leq \max_{\mathbb{L}^1 \in \mathcal{I}^1} \|\mathbf{H}^1\mathbf{A}_{\mathbb{L}^1}(\mathbf{x}_1 - \hat{\mathbf{x}}_1)\|^2 && (42)\\
&= |s_1 - \hat{s}_1|^2 \max_{1 \leq l_{1i} \leq p_d} \|\mathbf{h}^1_{l_{1i}}\|^2 \\
&\leq |s_1 - \hat{s}_1|^2 \sum_{k=1}^{p_d}\sum_{i=1}^{n_r} |h^1_{i,k}|^2. && (43)
\end{aligned}$$

Note that the set $\mathbb{L}^1_{\text{ED}}$ in (41) is dependent on $\mathbf{H}$, whereas the set $\mathbb{L}^1$ in (42) is independent of $\mathbf{H}$. The unconditional PEP between $\mathbf{x}$ and $\hat{\mathbf{x}}$ is given by

$$\begin{aligned}
P(\mathbf{x} \to \hat{\mathbf{x}}) &= \mathbb{E}_{\mathbf{H}}\left\{Q\left(\sqrt{\|\mathbf{H}\mathbf{A}_{\mathbb{L}_{\text{ED}}}(\mathbf{x} - \hat{\mathbf{x}})\|^2/2\sigma^2}\right)\right\} \\
&= \mathbb{E}_{\mathbf{H}}\left\{\frac{1}{\pi}\int_{\theta=0}^{\pi/2} \exp\left(-\frac{\|\mathbf{H}\mathbf{A}_{\mathbb{L}_{\text{ED}}}(\mathbf{x} - \hat{\mathbf{x}})\|^2}{4\sigma^2\sin^2(\theta)}\right) d\theta\right\} \\
&\geq \frac{1}{\pi}\int_{\theta=0}^{\pi/2} \mathbb{E}_{\mathbf{H}}\left\{\exp\left(\frac{-|s_1 - \hat{s}_1|^2}{4\sigma^2\sin^2(\theta)}\sum_{k=1}^{p_d}\sum_{i=1}^{n_r}|h^1_{i,k}|^2\right)\right\} d\theta. \quad (44)
\end{aligned}$$

Since $|h^1_{i,k}|^2$s are independent and exponentially distributed with unit mean, we have

$$P(\mathbf{x} \to \hat{\mathbf{x}}) \ \geq \ \frac{1}{\pi}\int_{\theta=0}^{\pi/2}\left(1 + \frac{|s_1 - \hat{s}_1|^2}{4\sigma^2\sin^2(\theta)}\right)^{-n_r p_d} d\theta. \tag{45}$$

Since $\frac{|s_1 - \hat{s}_1|^2}{4\sigma^2\sin^2(\theta)} \gg 1$ at high SNRs, we can write

$$P(\mathbf{x} \to \hat{\mathbf{x}}) \geq \left(\frac{|s_1 - \hat{s}_1|^2}{4\sigma^2}\right)^{-n_r p_d} \frac{1}{\pi}\int_{\theta=0}^{\pi/2} \sin^{2n_r p_d}(\theta) d\theta, \tag{46}$$

which shows the diversity order of $P(\mathbf{x} \to \hat{\mathbf{x}})$ is upper bounded by $n_r p_d = n_r\,(|\mathbb{S}_{\text{all}}| - |\mathbb{S}_{\text{sub}}| + 1)$, i.e., $d_{\mathbf{x},\hat{\mathbf{x}}} \leq n_r\,(|\mathbb{S}_{\text{all}}| - |\mathbb{S}_{\text{sub}}| + 1)$. From (30), an upper bound on d is obtained as

$$d = \min_{\mathbf{x} \neq \tilde{\mathbf{x}}} d_{\mathbf{x},\tilde{\mathbf{x}}} \ \leq \ d_{\mathbf{x},\hat{\mathbf{x}}} \ \leq \ n_r\,(|\mathbb{S}_{\text{all}}| - |\mathbb{S}_{\text{sub}}| + 1)\,. \tag{47}$$

Finally, from (40) and (47), we see that the diversity order (d) achieved by the ED-based MAP selection scheme is $n_r\,(|\mathbb{S}_{\text{all}}| - |\mathbb{S}_{\text{sub}}| + 1)$.

APPENDIX B
PROOF OF PROPOSITION 2

Proof: Let k^* be the solution to the optimization problem in (28) for a given realization $\tilde{\mathbf{h}}$, i.e., the k^*th receive antenna is selected. Let $d_{\text{pc-cr}}$ denote the diversity order achieved by PC-CR scheme. In the following, we derive upper and lower bounds on $d_{\text{pc-cr}}$ and show that these bounds turn out to be the same, given by $n_r(n_{tu} + 1)$.

1) Lower bound on $d_{pc\text{-}cr}$: Let $\triangle\mathbb{V}^k_{\text{pc-cr}}$ be the set of difference vectors corresponding to the set $\mathbb{V}^k_{\text{pc-cr}}$, i.e., $\triangle\mathbb{V}^k_{\text{pc-cr}} = \{\mathbf{v}_1 - \mathbf{v}_2 : \mathbf{v}_1, \mathbf{v}_2 \in \mathbb{V}^k_{\text{pc-cr}}, \mathbf{v}_1 \neq \mathbf{v}_2\}$. Let $\triangle\mathcal{D}$ be the set of matrices defined as $\triangle\mathcal{D} = \{\mathbf{D} = [\mathbf{B}_1\mathbf{d}_1 \ \mathbf{B}_2\mathbf{d}_2 \cdots \mathbf{B}_{n_r}\mathbf{d}_{n_r}] : \mathbf{d}_k \in \triangle\mathbb{V}^k_{\text{pc-cr}}, k = 1, \cdots, n_r\}$. The size of each matrix in $\triangle\mathcal{D}$ is $n_r n_{tu} N_m \times n_r$. The conditional BEP at high SNRs is given by

$$P_{B|\tilde{\mathbf{h}}} \approx P_{B|\tilde{\mathbf{h}}_{k^*}} \leq Q\left(\left(\min_{\substack{\mathbf{v}_1,\mathbf{v}_2 \in \mathbb{V}^{k^*}_{\text{pc-cr}} \\ \mathbf{v}_1 \neq \mathbf{v}_2}} \frac{|\tilde{\mathbf{h}}^T\mathbf{B}_{k^*}(\mathbf{v}_1 - \mathbf{v}_2)|^2}{2\sigma^2}\right)^{\frac{1}{2}}\right). \tag{48}$$

The inequality in (48) follows from $1 \leq \delta(\mathbf{v}_1, \mathbf{v}_2) \leq \eta$. Let $\mathbf{d}^{\min}_k = \text{argmin}_{\mathbf{d} \in \triangle\mathbb{V}^k_{\text{pc-cr}}} |\tilde{\mathbf{h}}^T\mathbf{B}_k\mathbf{d}|^2$ for $1 \leq k \leq n_r$ denote the difference vector from $\triangle\mathbb{V}^k_{\text{pc-cr}}$ corresponding to the minimum ED. We then have

$$\begin{aligned}
P_{B|\tilde{\mathbf{h}}} &\leq Q\left(\sqrt{\frac{|\tilde{\mathbf{h}}^T\mathbf{B}_{k^*}\mathbf{d}^{\min}_{k^*}|^2}{2\sigma^2}}\right) \leq \frac{1}{2}\exp\left(\frac{-|\tilde{\mathbf{h}}^T\mathbf{B}_{k^*}\mathbf{d}^{\min}_{k^*}|^2}{4\sigma^2}\right) && (49)\\
&\leq \ \frac{1}{2}\exp\Big(\frac{-1}{4n_r\sigma^2}\sum_{i=1}^{n_r}|\tilde{\mathbf{h}}^T\mathbf{B}_i\mathbf{d}^{\min}_i|^2\Big) && (50)\\
&= \ \frac{1}{2}\prod_{i=1}^{n_r}\exp\Big(-\frac{1}{4\hat{\sigma}^2}|\tilde{\mathbf{h}}^T_i\mathbf{d}^{\min}_i|^2\Big),
\end{aligned}$$

where $\hat{\sigma}^2 = n_r\sigma^2$. The second inequality in (49) follows from Chernoff bound and the inequality in (50) is due to the fact that $\mathbf{d}^{\min}_{k^*}$ corresponds to the maximum ED among the elements $\{\mathbf{d}^{\min}_k\}_{k=1}^{n_r}$. The average BEP at high SNRs is then given by

$$\begin{aligned}
P_B \ &\approx \ \mathbb{E}_{\tilde{\mathbf{h}}}\{P_{B|\tilde{\mathbf{h}}}\} \leq \frac{1}{2}\mathbb{E}_{\tilde{\mathbf{h}}}\left\{\prod_{i=1}^{n_r}\exp\Big(-\frac{1}{4\hat{\sigma}^2}|\tilde{\mathbf{h}}^T_i\mathbf{d}^{\min}_i|^2\Big)\right\} \\
&= \frac{1}{2}\underbrace{\left(\mathbb{E}_{\tilde{\mathbf{h}}_1}\left\{\exp\left(\frac{-1}{4\hat{\sigma}^2}|\tilde{\mathbf{h}}^T_1\mathbf{d}^{\min}_1|^2\right)\right\}\right)^{n_r}}_{\triangleq P_{BU}} = \frac{1}{2}\left(P_{BU}\right)^{n_r}, \quad (51)
\end{aligned}$$

where the equality in (51) follows from the independent and identical distribution of $\tilde{\mathbf{h}}_i$s. Next, we show that the diversity order of P_{BU} is lower bounded by $n_{tu}+1$.

Diversity order of P_{BU}: Let $d_{\mathbf{v}_k,\mathbf{v}_{k'}}$ denote the diversity order of PEP $P(\mathbf{v}_k \to \mathbf{v}_{k'})$. The codeword error probability (CEP) can be approximated by applying nearest neighbor approximation in the high SNR region ([44], Eq. 5.45), as

$$\sum_{\mathbf{v}_k}\sum_{\mathbf{v}_{k'}\neq\mathbf{v}_k} P(\mathbf{v}_k \to \mathbf{v}_{k'}) \approx \mathbb{E}_{\tilde{\mathbf{h}}_1}\left\{Q\left(\sqrt{\frac{|\tilde{\mathbf{h}}_1^T\mathbf{d}_1^{\min}|^2}{2\hat{\sigma}^2}}\right)\right\} \approx \frac{P_{BU}}{2}. \quad (52)$$

From (52), the diversity order of P_{BU}, denoted by d_{BU}, is given by $\min_{\mathbf{v}_k\neq\mathbf{v}_{k'}} d_{\mathbf{v}_k,\mathbf{v}_{k'}}$. Let l_{j_k} denote the index of the MAP chosen on the jth MBM-TU in the transmit vector $\mathbf{v}_k$, i.e., l_{j_k} is the index of the non-zero entry in the vector $[v^k_{(j-1)N_m+1} \;\; v^k_{(j-1)N_m+2} \;\; \cdots \;\; v^k_{jN_m}]$. Let $\mathbb{G}^c_{k,k'}$ denote the set defined as $\mathbb{G}^c_{k,k'} \triangleq \{j : l_{j_k} = l_{j_{k'}}, j = 1,\cdots,n_{tu}\}$, i.e., set of js for which l_{j_k} and $l_{j_{k'}}$ are same. Likewise, let $\mathbb{G}^d_{k,k'}$ denote the set defined as $\mathbb{G}^d_{k,k'} \triangleq \{j : l_{j_k} \neq l_{j_{k'}}, j = 1,\cdots,n_{tu}\}$, i.e., set of js for which l_{j_k} and $l_{j_{k'}}$ are different. Note that, for any $k \neq k'$, $|\mathbb{G}^c_{k,k'}| + |\mathbb{G}^d_{k,k'}| = n_{tu}$, and $0 \leq |\mathbb{G}^c_{k,k'}| \leq n_{tu}-1$. Now, the PEP between $\mathbf{v}_k$ and $\mathbf{v}_{k'}$ is given by

$$\begin{aligned} P(\mathbf{v}_k \to \mathbf{v}_{k'}) &= \mathbb{E}_{\tilde{\mathbf{h}}_1}\left\{Q\left(\sqrt{|\tilde{\mathbf{h}}_1^T(\mathbf{v}_k-\mathbf{v}_{k'})|^2/2\hat{\sigma}^2}\right)\right\} \\ &= \mathbb{E}_{\tilde{\mathbf{h}}_1}\left\{Q\left(\left(\frac{1}{2\hat{\sigma}^2}\Big|\sum_{j=1}^{n_{tu}} |h^j_{1,l_{j_k}}|e^{\imath\psi_k} - |h^j_{1,l_{j_{k'}}}|e^{\imath\psi_{k'}}\Big|^2\right)^{\frac{1}{2}}\right)\right\} \\ &= \mathbb{E}_{\tilde{\mathbf{h}}_1}\left\{Q\left(\sqrt{(t_c+t_d+\Delta)/2\hat{\sigma}^2}\right)\right\}, \end{aligned} \quad (53)$$

where $t_c = S_cP_c$, $t_d = S^k_d + S^{k'}_d - 2S^d_kS^d_{k'}\cos(\psi_{k,k'})$, $\Delta = 2\big(S^c(S^d_k + S^d_{k'})(1-\cos(\psi_{k,k'})) + \sum_{j\in\mathbb{G}^c_{k,k'}}\sum_{j'\neq j\in\mathbb{G}^c_{k,k'}} |h^j_{1,l_{j_k}}||h^{j'}_{1,l_{j'_k}}|P_c + \sum_{j\in\mathbb{G}^d_{k,k'}}\sum_{j'\neq j\in\mathbb{G}^d_{k,k'}}\big(|h^j_{1,l_{j_k}}||h^{j'}_{1,l_{j'_k}}| + |h^j_{1,l_{j_{k'}}}||h^{j'}_{1,l_{j'_{k'}}}|\big)\big)$, $S_c = \sum_{j\in\mathbb{G}^c_{k,k'}}|h^j_{1,l_{j_k}}|^2$, $P_c = |e^{\imath\psi_k} - e^{\imath\psi_{k'}}|^2$, $S^k_d = \sum_{j\in\mathbb{G}^d_{k,k'}}|h^j_{1,l_{j_k}}|^2$, $S^{k'}_d = |h^j_{1,l_{j_{k'}}}|^2$, $S^d_k = \sum_{j\in\mathbb{G}^d_{k,k'}}|h^j_{1,l_{j_k}}|$, $S^d_{k'} = \sum_{j\in\mathbb{G}^d_{k,k'}}|h^j_{1,l_{j_{k'}}}|$, $S^c = \sum_{j\in\mathbb{G}^c_{k,k'}}|h^j_{1,l_{j_k}}|$, and $\psi_{k,k'} = \psi_k - \psi_{k'}$. Since $\Delta \geq 0$, we have

$$\begin{aligned} P(\mathbf{v}_k \to \mathbf{v}_{k'}) &\leq \mathbb{E}_{\tilde{\mathbf{h}}_1}\left\{Q\left(\sqrt{(t_c+t_d)/2\hat{\sigma}^2}\right)\right\} \\ &\leq \mathbb{E}_{\tilde{\mathbf{h}}_1}\left\{\frac{1}{2}\exp\Big(-(t_c+t_d)/4\hat{\sigma}^2\Big)\right\} \quad (54) \\ &= \frac{1}{2}\underbrace{\mathbb{E}_{\tilde{\mathbf{h}}_1}\{\exp(\tfrac{-t_c}{4\hat{\sigma}^2})\}}_{\triangleq\, T_c}\underbrace{\mathbb{E}_{\tilde{\mathbf{h}}_1}\{\exp(\tfrac{-t_d}{4\hat{\sigma}^2})\}}_{\triangleq\, T_d} = \frac{1}{2}T_cT_d, \quad (55) \end{aligned}$$

where the inequality in (54) follows from Chernoff bound and the equality in (55) follows from independence of $\{h^j_{1,l_{j_k}} \in \mathbb{G}^c_{k,k'}\}$ and $\{h^j_{1,l_{j_k}}, h^j_{1,l_{j_{k'}}} \in \mathbb{G}^d_{k,k'}\}$. Now, since $|h^j_{1,l_{j_k}}|^2$s are independent and exponentially distributed with unit mean, from (55), T_c can be written as

$$T_c = \mathbb{E}_{\tilde{\mathbf{h}}_1}\left\{\exp\left(\frac{-P_c}{4\hat{\sigma}^2}\sum_{j\in\mathbb{G}^c_{k,k'}}|h^j_{1,l_{j_k}}|^2\right)\right\} = \left(1+\frac{P_c}{4\hat{\sigma}^2}\right)^{-|\mathbb{G}^c_{k,k'}|}.$$

Since $\frac{P_c}{4\hat{\sigma}^2} \gg 1$ at high SNRs, we can approximate T_c as

$$T_c \;\approx\; (P_c/4)^{-|\mathbb{G}^c_{k,k'}|}\big(1/\hat{\sigma}^2\big)^{-(|\mathbb{G}^c_{k,k'}|)}. \quad (56)$$

Similarly, from (55), T_d can be written as

$$\begin{aligned} T_d &= \mathbb{E}_{\tilde{\mathbf{h}}_1}\Big\{\exp\Big(\frac{-1}{4\hat{\sigma}^2}\big(S^k_d + S^{k'}_d - 2S^k_dS^d_{k'}\cos(\psi_{k,k'})\big)\Big)\Big\} \\ &\leq \mathbb{E}_{\tilde{\mathbf{h}}_1}\Big\{\exp\Big(\frac{-1}{4\hat{\sigma}^2}\big(S^k_d + S^{k'}_d - 2|\mathbb{G}^d_{k,k'}|\big(S^k_dS^{k'}_d\big)^{\frac{1}{2}}\cos(\psi_{k,k'})\big)\Big)\Big\}, \quad (57) \end{aligned}$$

where the inequality in (57) follows from Cauchy-Schwartz inequalities given by $S^d_k \leq \big(|\mathbb{G}^d_{k,k'}|S^k_d\big)^{\frac{1}{2}}$ and $S^d_{k'} \leq \big(|\mathbb{G}^d_{k,k'}|S^{k'}_d\big)^{\frac{1}{2}}$. Let $p = (S^k_d)^{0.5}$ and $q = (S^{k'}_d)^{0.5}$. Note that p and q are central Chi distributed with $2|\mathbb{G}^d_{k,k'}|$ degrees of freedom. Therefore, (57) can be written as

$$T_d \leq \int_{p=0}^{\infty}\int_{q=0}^{\infty} e^{\frac{-(p^2+q^2-2pq\cos(\psi_{k,k'}))}{4\hat{\sigma}^2}}\frac{(pq)^{2|\mathbb{G}^d_{k,k'}|-1}e^{\frac{-(p^2+q^2)}{2}}}{4^{|\mathbb{G}^d_{k,k'}|-1}(\Gamma(|\mathbb{G}^d_{k,k'}|))^2}dp\,dq,$$

where $\Gamma(.)$ denotes the Gamma function. Substituting $p = r\cos\theta$ and $q = r\sin\theta$, we have

$$\begin{aligned} T_d &\leq \int_{\theta=0}^{\frac{\pi}{2}}\frac{8\sin^{2|\mathbb{G}^d_{k,k'}|-1}(2\theta)}{\Gamma(|\mathbb{G}^d_{k,k'}|)^2 2^{4|\mathbb{G}^d_{k,k'}|}}\int_{r=0}^{\infty} e^{-\frac{r^2}{4\hat{\sigma}^2}\left(1+2\hat{\sigma}^2-\sin(2\theta)\cos(\psi_{k,k'})\right)} r^{4\left|\mathbb{G}^d_{k,k'}\right|-1}dr\,d\theta \\ &= \int_{\theta=0}^{\frac{\pi}{2}}4\frac{\Gamma(2|\mathbb{G}^d_{k,k'}|)}{\Gamma(|\mathbb{G}^d_{k,k'}|)^2}\left(\frac{1+2\hat{\sigma}^2-\sin(2\theta)\cos(\psi_{k,k'})}{\sin(2\theta)\hat{\sigma}^2}\right)^{-2|\mathbb{G}^d_{k,k'}|}\sin^{-1}(2\theta)\,d\theta. \end{aligned}$$

Since $1 \gg 2\hat{\sigma}^2$ at high SNRs, we can write

$$\begin{aligned} T_d \;&\leq\; \big(1/\hat{\sigma}^2\big)^{-2|\mathbb{G}^d_{k,k'}|} \\ &\underbrace{\int_{\theta=0}^{\frac{\pi}{2}}4\frac{\Gamma(2|\mathbb{G}^d_{k,k'}|)}{\Gamma(|\mathbb{G}^d_{k,k'}|)^2}\left(\frac{1-\sin(2\theta)\cos(\psi_{k,k'})}{\sin(2\theta)}\right)^{-2|\mathbb{G}^d_{k,k'}|}\sin^{-1}(2\theta)\,d\theta}_{\triangleq k_d}. \quad (58) \end{aligned}$$

Note that k_d is independent of $\hat{\sigma}^2$. Now, from (55), (56), (58), we can write

$$P(\mathbf{v}_k \to \mathbf{v}_{k'}) \leq \frac{k_d}{2}\left(\frac{P_c}{4}\right)^{-|\mathbb{G}^c_{k,k'}|}\left(\frac{1}{\hat{\sigma}^2}\right)^{-(|\mathbb{G}^c_{k,k'}|+2|\mathbb{G}^d_{k,k'}|)}, \quad (59)$$

which shows that the diversity order $d_{\mathbf{v}_k,\mathbf{v}_{k'}} \geq |\mathbb{G}^c_{k,k'}| + 2|\mathbb{G}^d_{k,k'}|$. Hence, the diversity order of P_{BU} is $d_{BU} = \min_{\mathbf{v}_k\neq\mathbf{v}_{k'}} d_{\mathbf{v}_k,\mathbf{v}_{k'}} \geq \min_{\mathbf{v}_k\neq\mathbf{v}_{k'}}|\mathbb{G}^c_{k,k'}| + 2|\mathbb{G}^d_{k,k'}|$. Since $|\mathbb{G}^c_{k,k'}| + |\mathbb{G}^d_{k,k'}| = n_{tu}$ for any $k \neq k'$, the minimum value for $|\mathbb{G}^c_{k,k'}| + 2|\mathbb{G}^d_{k,k'}| = 2n_{tu} - |\mathbb{G}^c_{k,k'}|$ is obtained when $|\mathbb{G}^c_{k,k'}|$ is maximum. That is, $\min_{k\neq k'}|\mathbb{G}^c_{k,k'}| + 2|\mathbb{G}^d_{k,k'}| = 2n_{tu} - \max_{k\neq k'}|\mathbb{G}^c_{k,k'}|$. Also, since $0 \leq |\mathbb{G}^c_{k,k'}| \leq n_{tu}-1$ for any $k \neq k'$, $\max_{k\neq k'}|\mathbb{G}^c_{k,k'}| = n_{tu}-1$. Hence, $\min_{k\neq k'}|\mathbb{G}^c_{k,k'}| + 2|\mathbb{G}^d_{k,k'}| = 2n_{tu} - (n_{tu}-1) = n_{tu}+1$, which gives $d_{BU} \geq n_{tu}+1$. Therefore, from (51), the diversity order achieved by the PC-CR scheme is lower bounded as

$$d_{\text{pc-cr}} \;\geq\; n_r d_{BU} \;\geq\; n_r(n_{tu}+1). \quad (60)$$

2) Upper bound on $d_{pc\text{-}cr}$: Consider a pair of transmitted vectors $\mathbf{v}_k, \hat{\mathbf{v}}_{k'}$ such that $|\mathbb{G}^c_{k,k'}| = n_{tu}-1$. Without loss of generality, assume $\mathbb{G}^c_{k,k'} = \{1,\; 2,\; \cdots,\; n_{tu}-1\}$. We have

$$|\tilde{\mathbf{h}}^T_{k^*}(\mathbf{v}_k - \hat{\mathbf{v}}_{k'})|^2 \;\leq\; \sum_{i=1}^{n_r}|\tilde{\mathbf{h}}^T_i(\mathbf{u}_ke^{\imath\psi_k} - \hat{\mathbf{u}}_{k'}e^{\imath\psi_{k'}})|^2$$

$$\leq \sum_{i=1}^{n_r} |\tilde{\mathbf{h}}_i^T(\mathbf{u}_k + \hat{\mathbf{u}}_{k'})|^2 \quad (61)$$

$$= \sum_{i=1}^{n_r} \left(2 \sum_{j=1}^{n_{tu}-1} |h_{i,l_{j_k}}^j| + |h_{1,i_{n_{tu}k}}^{n_{tu}}| + |h_{i,l_{n_{tu}k'}}^{n_{tu}}|\right)^2$$

$$\leq (4n_{tu}-2)\sum_{i=1}^{n_r}\sum_{j=1}^{n_{tu}-1}|h_{i,l_{j_k}}^j|^2+|h_{i,l_{n_{tu}k}}^{n_{tu}}|^2+|h_{i,l_{n_{tu}k'}}^{n_{tu}}|^2, \quad (62)$$

where the inequality in (61) follows from the fact that the distance between two points is maximum when phase difference between them is π, and the inequality in (62) follows from Cauchy-Schwartz inequality. Now, using (62) and following similar derivation steps in Eqs. (44)-(46) in Appendix A, the unconditional PEP between $\mathbf{v}_k$ and $\hat{\mathbf{v}}_{k'}$, $P(\mathbf{v}_k \to \hat{\mathbf{v}}_{k'})$, can be obtained as

$$P(\mathbf{v}_k \to \hat{\mathbf{v}}_{k'}) = \mathbb{E}_{\mathbf{H}}\left\{Q\left(\sqrt{|\tilde{\mathbf{h}}_{k*}^T(\mathbf{v}_k - \hat{\mathbf{v}}_{k'})|^2/2\sigma^2}\right)\right\}$$

$$\geq \left(\frac{4n_{tu}-2}{4\sigma^2}\right)^{-n_r(n_{tu}+1)} \frac{1}{\pi}\int_{\theta=0}^{\frac{\pi}{2}} \sin^{2n_r(n_{tu}+1)}(\theta)d\theta, \quad (63)$$

which shows that the diversity order of $P(\mathbf{v}_k \to \hat{\mathbf{v}}_{k'})$ is upper bounded by $n_r(n_{tu}+1)$, i.e., $d_{\mathbf{v}_k,\hat{\mathbf{v}}_{k'}} \leq n_r(n_{tu}+1)$. Therefore, we have

$$d_{\text{pc-cr}} = \min_{\mathbf{v}_k \neq \mathbf{v}_{k'}} d_{\mathbf{v}_k,\mathbf{v}_{k'}} \leq d_{\mathbf{v}_k,\hat{\mathbf{v}}_{k'}} \leq n_r(n_{tu}+1). \quad (64)$$

From (60) and (64), we see that the diversity order ($d_{\text{pc-cr}}$) achieved by the PC-CR scheme is $n_r(n_{tu}+1)$.

ACKNOWLEDGMENT

The authors would like to thank Prof. Arogyaswami Paulraj, Stanford University for the insightful discussions on the use of parasitic elements in smart antenna systems.

REFERENCES

[1] Y. A. Chau and S.-H. Yu, "Space modulation on wireless fading channels," in *Proc. IEEE 54th VTC'2001 (Fall)*, vol. 3, Oct. 2001, pp. 1668-1671.

[2] J. Jeganathan, A. Ghrayeb, L. Szczecinski, and A. Ceron, "Space shift keying modulation for MIMO channels," *IEEE Trans. Wireless Commun.,* vol. 8, no. 7, pp. 3692-3703, Jul. 2009.

[3] A. K. Khandani, "Media-based modulation: A new approach to wireless transmission," in *Proc. IEEE ISIT'2013*, Jul. 2013, pp. 3050-3054.

[4] A. K. Khandani, "Media-based modulation: Converting static Rayleigh fading to AWGN," in *Proc. IEEE ISIT'2014*, Jun.-Jul. 2014, pp. 1549-1553.

[5] A. K. Khandani, "Media-based modulation: A new approach to wireless transmission," Tech. Rep., University of Waterloo, Canada. Online: http://www.cst.uwaterloo.ca/reports/media-report.pdf

[6] J. Jeganathan, A. Ghrayeb, and L. Szczecinski, "Generalized space shift keying modulation for MIMO channels," in *Proc. IEEE PIMRC'2008*, Sep. 2008, pp. 1-5.

[7] E. Seifi, M. Atamanesh, and A. K. Khandani, "Media-based modulation: A new frontier in wireless communications," online: arXiv:1507.07516v3 [cs.IT] 7 Oct. 2015.

[8] R. Mesleh, H. Haas, S. Sinanovic, C. W. Ahn, and S. Yun, "Spatial modulation," *IEEE Trans. Veh. Tech.*, vol. 57, no. 4, pp. 2228-2241, Jul. 2008.

[9] M. Di Renzo, H. Haas, A. Ghrayeb, S. Sugiura, and L. Hanzo, "Spatial modulation for generalized MIMO: Challenges, opportunities and implementation," *Proceedings of the IEEE*, vol. 102, no. 1, pp. 56-103, Jan. 2014.

[10] A. Chockalingam and B. S. Rajan, *Large MIMO Systems*, Cambridge Univ. Press, Feb. 2014.

[11] J. Wang, S. Jia, and J. Song, "Generalised spatial modulation system with multiple active transmit antennas and low complexity detection scheme," *IEEE Trans. Wireless Commun.*, vol. 11, no. 4, pp. 1605-1615, Apr. 2012.

[12] T. Datta and A. Chockalingam, "On generalized spatial modulation," in *Proc. IEEE WCNC'2013*, Apr. 2013, pp. 2716-2721.

[13] T. Lakshmi Narasimhan and A. Chockalingam, "On the capacity and performance of generalized spatial modulation," *IEEE Commun. Lett.*, vol. 20, no. 2, pp. 252-255, Feb. 2016.

[14] P. Som and A. Chockalingam, "Spatial modulation and space shift keying in single carrier communication," in *Proc. IEEE PIMRC'2012*, Sep. 2012, pp. 1962-1967.

[15] R. Rajashekar, K. V. S. Hari, and L. Hanzo, "Spatial modulation aided zero-padded single carrier transmission for dispersive channels," *IEEE Trans. Commun.*, vol. 61, no. 6, pp. 2318-2329, Jun. 2013.

[16] L. Xiao, L. Dan, Y. Zhang, Y. Xiao, P. Yang, and S. Li, "A low-complexity detection scheme for generalized spatial modulation aided single carrier systems," *IEEE Commun. Lett.*, vol. 19, no. 6, pp. 1069-1072, Jun. 2015.

[17] P. Yang et al., "Single-carrier spatial modulation: a promising design for large scale broadband antenna systems," *IEEE Commun. Surveys & Tuts.*, vol. 18, no. 3, pp. 1687-1715, 3rd Quarter 2016.

[18] R. Abu-alhiga and H. Haas, "Subcarrier index modulation OFDM," in *Proc. IEEE PIMRC'2009*, Sep. 2009, pp. 177-181.

[19] E. Basar, U. Aygolu, E. Panayirci, and H. V. Poor, "Orthogonal frequency division multiplexing with indexing," in *Proc. IEEE GLOBECOM'2012*, Dec. 2012, pp. 4741-4746.

[20] Y. Xiao, S. Wang, L. Dan, X. Lei, P. Yang, and W. Xiang, "OFDM with interleaved subcarrier-index modulation," *IEEE Commun. Lett.*, vol. 8, no. 8, pp. 1447-1450, Aug. 2014.

[21] T. Datta, H. Eshwaraiah, and A. Chockalingam, "Generalized space and frequency index modulation," *IEEE Trans. Veh. Tech.*, vol. 65, no. 7, pp. 4911-4924, Jul. 2016.

[22] T. Lakshmi Narasimhan, Y. Naresh, T. Datta, and A. Chockalingam, "Pseudo-random phase precoded spatial modulation and precoder index modulation," in *Proc. IEEE GLOBECOM'2014*, Nov. 2014, pp. 3868-3873.

[23] B. Schaer, K. Rambabu, J. Borneman, and R. Vahldieck, "Design of reactive parasitic elements in electronic beam steering arrays," *IEEE Trans. Ant. and Propagat.*, vol. 53, no. 6, pp. 1998-2003, Jun. 2005.

[24] R. Vaughan, "Switched parasitic elements for antenna diversity," *IEEE Trans. Ant. and Propagat.*, vol. 47, no. 2, pp. 399-405, Feb. 1999.

[25] S. L. Preston, D. V. Thiel, T. A. Smith, S. G. OKeefe, and J. W. Lu, "Base-station tracking in mobile communications using a switched parasitic antenna array," *IEEE Trans. Ant. and Propagat.*, vol. 46, no. 6, pp. 841-844, Jun. 1998.

[26] C. Sun and N. C. Karmakar, "Direction of arrival estimation with a novel single-port smart antenna," *EURASIP J. Applied Signal Process.*, 2004, 2004:9, 1364-1375.

[27] C. G. Christodoulou, Y. Tawk, S. A. Lane, and S. R. Erwin, "Reconfigurable antennas for wireless and space applications," *Proceedings of the IEEE*, vol. 100, no. 7, pp. 2250-2261, Jul. 2012.

[28] J. Costantine, Y. Tawk, S. E. Barbin, and C. G. Christodoulou, "Reconfigurable antennas: design and applications," *Proceedings of the IEEE*, vol. 103, no. 3, pp. 424-437, Mar. 2015.

[29] O. N. Alrabadi, A. Kalis, C. B. Papadias, R. Prasad, "Aerial modulation for high order PSK transmission schemes," in *Wireless VITAE 2009*, May 2009, pp. 823-826.

[30] O. N. Alrabadi, A. Kalis, C. B. Papadias, and R. Prasad, "A universal encoding scheme for MIMO transmission using a single active element for PSK modulation schemes," *IEEE Trans. Wireless Commun.*, vol. 8 , no. 10, pp. 5133-5142, Oct. 2009.

[31] R. Bains, "On the usage of parasitic antenna elements in wireless communication systems," Ph.D. Thesis, Department of Electronics and Telecommunications, Norwegian University of Science and Technology, May 2008. Online: http://ntnu.diva-portal.org/smash/get/diva2:124527/FULLTEXT01.pdf

[32] Y. Naresh and A. Chockalingam, "On media-based modulation using RF mirrors," in *Proc. ITA'2016*, San Diego, Feb. 2016.

[33] M.-S. Alouini and A. Goldsmith, "A unified approach for calculating error rates of linearly modulated signals over generalized fading channels," *IEEE Trans. Commun.*, vol. 47, no. 9, pp. 1324-1334, Sep. 1999.

[34] R. Mesleh, M. D. Renzo, H. Haas, and P. M. Grant, "Trellis coded spatial modulation," *IEEE Trans. Wireless Commun.*, vol. 9 , no. 7, pp. 2349-2361, Jul. 2010.

[35] S. Lokya, " Channel capacity of MIMO architecture using the exponential correlation matrix," *IEEE Commun. Lett*., vol. 5, no. 9, pp. 369-371, Sep. 2001.
[36] E. Basar, U. Aygolu, E. Panayirci, and H. V. Poor, " New trellis code design for spatial modulation," *IEEE Trans. Wireless Commun.*, vol. 10 , no. 8, pp. 2670-2680, Aug. 2011.
[37] R. Rajashekar, K. V. S. Hari, and L. Hanzo, "Antenna selection in spatial modulation systems," *IEEE Commun. Lett*., vol. 17, no. 3, pp. 521-524, Mar. 2013.
[38] P. Yang, Y. Xiao, Y. Li, and S. Li, "Adaptive spatial modulation for wireless MIMO transmission systems," *IEEE Commun. Lett.*, vol. 15, no. 6, pp. 602-604, Jun. 2011.
[39] P. Yang, M. Di Renzo, Y. Xiao, S. Li, and L. Hanzo, "Design guidelines for spatial modulation," *IEEE Commun. Surveys Tuts.*, vol. 17, no. 1, pp. 6-26, 2015.
[40] R. Rajashekar, K. V. S. Hari, and L. Hanzo, "Quantifying the transmit diversity order of Euclidean distance based antenna selection in spatial modulation," *IEEE Signal. Process. Lett.*, vol. 22, no. 9, pp. 1434-1437, Sep. 2015.
[41] X. Jin and D. Cho, "Diversity analysis on transmit antenna selection for spatial multiplexing systems with ML detection," *IEEE Trans. Veh. Tech.*, vol. 62, no. 9, pp. 4653-4658, Nov. 2013.
[42] K. Ntontin, M. Di Renzo, A. Perez-Neira, and C. Verikoukis, "Adaptive generalized space shift keying," *EURASIP J. Wireless Commun. and Netw.*, 2013, 2013:43.
[43] M. S. Veedu, C. R. Murthy, and L. Hanzo, "Single-RF spatial modulation relying on finite-rate phase-only feedback: Design and analysis," *IEEE Trans. Veh. Tech.*, vol. 65, no. 4, pp. 2016-2025, Apr. 2016.
[44] A. Goldsmith, *Wireless Communications*, Cambridge Univ. Press, 2005.

Y. Naresh received the B.E. degree in electronics and communication engineering from Osmania University, Hyderabad, India, in 2012 and the M.E. degree in electrical communication engineering from the Indian Institute of Science, Bangalore, India, in 2014. He is currently pursuing the Ph.D. degree in electrical communication engineering at the Indian Institute of Science, Bangalore. His current research interests include index modulation, low-complexity implementation and performance analysis of wireless communication systems.

A. Chockalingam (S'92-M'93-SM'98) was born in Rajapalayam, Tamil Nadu, India. He received the B.E. (Honors) degree in electronics and communication engineering from the PSG College of Technology, Coimbatore, India, in 1984; the M.Tech. degree in electronics and electrical communication engineering (with specialization in satellite communications) from the Indian Institute of Technology, Kharagpur, India, in 1985; and the Ph.D. degree in electrical communication engineering (ECE) from the Indian Institute of Science (IISc), Bangalore, India, in 1993. From 1986 to 1993, he worked with the Transmission R&D division, Indian Telephone Industries Limited, Bangalore. From December 1993 to May 1996, he was a Postdoctoral Fellow and an Assistant Project Scientist with the Department of Electrical and Computer Engineering, University of California, San Diego, CA, USA. From May 1996 to December 1998, he was with Qualcomm, Inc., San Diego, as a Staff Engineer/Manager in the Systems Engineering Group. Since December 1998, he has been with the faculty of the Department of ECE, IISc, Bangalore, where he is a Professor, working in the area of wireless communications and networking.

Dr. Chockalingam served as an Associate Editor for the IEEE TRANSACTIONS ON VEHICULAR TECHNOLOGY, as an Editor for the IEEE TRANSACTIONS ON WIRELESS COMMUNICATIONS, and as a Guest Editor for the IEEE JOURNAL ON SELECTED AREAS IN COMMUNICATIONS (Special Issue on Multiuser Detection for Advanced Communication Systems and Networks) and for the IEEE JOURNAL OF SELECTED TOPICS IN SIGNAL PROCESSING (Special Issue on Soft Detection on Wireless Transmission). He received the Swarnajayanti Fellowship and the J. C. Bose National Fellowship from the Department of Science and Technology, Government of India. He is a Fellow of the Indian National Academy of Engineering; the National Academy of Sciences, India; the Indian National Science Academy; and the Indian Academy of Sciences.